Grid-Connected PV + Battery AC Nano-grid with EV Integration for Increased Resilience

Mohammadali Ghaderi

A Thesis

in

The Department

of

Electrical and Computer Engineering

Presented in Partial Fulfillment of the Requirements

for the Degree of

Master of Applied Science (Electrical and Computer Engineering)

at Concordia University

Montréal, Québec, Canada

April 2025

©Mohammadali Ghaderi, 2025

CONCORDIA UNIVERSITY
SCHOOL OF GRADUATE STUDIES

This is to certify that the thesis prepared

By: Mohammadali Ghaderi

Entitled: Grid-Connected PV + Battery AC Nano-grid with EV Integration for Increased Resilience

and submitted in partial fulfillment of the requirements for the degree of

Master of Applied Science (Electrical and Computer Engineering)

complies with the regulations of this University and meets the accepted standards with respect to originality and quality.

Signed by the final examining committee:

________________________________ Chair
Dr. Pragasen Pillay

________________________________ Internal Examiner
Dr. Pragasen Pillay

________________________________External Examiner
Dr. Hua Ge

________________________________ Internal Examiner
Dr. Luiz A. C. Lopes

Approved by: ____________________________________
Dr. Yusef R. Shayan, Chair
Department of Electrical and Computer Engineering

May 12, 2025 ____________________________________
Dr. Mourad Debbabi, Dean,
Faculty of Engineering and Computer Science

ABSTRACT

Grid-Connected PV + Battery AC Nano-grid with EV Integration for Increased Resilience

Mohammadali Ghaderi

This work presents a methodology for integrating a single-phase V2H/V2L inverter into a three-phase nano-grid equipped with photovoltaic (PV) generation and battery storage. The existing system, based on SMA technology, includes three Sunny Boys (SBs) and three Sunny Islands (SIs), all managed by a Data Manager (DM). Due to the inability of the V2H inverter to directly connect to the three-phase system, a novel scheme was developed, incorporating a spare SI, an ioLogik interface, relays, and an alarm system.

The proposed setup enables load shedding and allows the stationary battery to be supplemented with energy from the electric vehicle (EV), effectively extending the supply duration for high priority loads during grid faults or islanded conditions. The control logic is based on the state of charge (SoC) of the stationary battery. This strategy ensures a balance between maintaining power supply to critical loads (priority and higher priority loads) and conserving the EV's stored energy for critical situations.

The comprehensive experimental setup developed in this work, along with the adopted energy management strategy, was successfully tested, demonstrating its functionality. Furthermore, an alternative scheme and a V2G (Vehicle-to-Grid) configuration were explored to highlight the versatility of this methodology. The system's flexibility allows the integration of additional energy sources, such as fuel cells, wind turbines, and extra PV systems, by connecting them to the DC bus, providing a robust framework for advanced energy systems and energy management.

به نام خدا

Acknowledgment

I would like to express my heartfelt gratitude to my supervisor, Professor, Luiz A. C. Lopes for granting me the opportunity to delve deeper into science under his invaluable guidance and support.

I am deeply appreciative of the friendship and guidance provided by Dr. Akrem Aljehaimi. Their insights and advice were instrumental.

I extend my warm thanks to my colleagues in the PEER group laboratory for creating a supportive, home-like environment. Special thanks to Jay, Rao, Amir, Paul, Soliha, Nazanin, Neetusha, Bassam, Dr. Hyacinthe, Abraham, Hani and Kenneth for their camaraderie and encouragement.

I wish to express my profound appreciation to my parents, Reza and Sima, and my brother, Vahid, for their unwavering love, support, and inspiration throughout this journey.

Lastly, I would like to express my deepest gratitude to my wife and son for their unwavering patience, love, and support throughout my journey in pursuing this degree. Their encouragement and understanding have been my greatest source of strength, and I couldn't have achieved this milestone without them.

Table of Contest

List of Figures

List of Tables

Nomenclature

BIPV	Building Integrated Photovoltaics
BMS	Battery Management System
DM	SMA Data Manager M
DG	Distributed Generation
DER	Distributed Energy Resource
DOD	Depth of Discharge
EMS	Energy Management System
EV	Electric Vehicle
FBL	Future Building Laboratory
HRES	Hybrid Renewable Energy System
ioLogik	Moxa ioLogik E1242
MPPT	Maximum Power Point Tracking
NZEB	Net Zero Energy Building
PHEV	plug-in hybrid electric vehicle
RES	Renewable Energy Sources
SB	SMA Sunny Boy
SI	SMA Sunny Island
SOC	State of Charge
STPV	Semi-Transparent Photovoltaics
UPS	Uninterruptable Power Supply
V2G	Vehicle-to-Grid
V2H	Vehicle-to-House
V2L	Vehicle-to-Load

V2X	Vehicle-to-Everything

Chapter 1 - Introduction

1.1 Introduction

The introductory chapter aims to highlight the significance of this research work by providing a concise background on the integration of renewable energy systems in buildings, the role of electric vehicles (EVs), and their interaction with the electrical grid, buildings, and homes. This sets the stage for understanding the broader context and potential impact of the research.

Subsequent chapters will provide a detailed description of the developed test setup and a discussion of the test results, demonstrating the feasibility and benefits of the proposed energy management strategies.

1.2 Environmental Concerns

Environmental concerns regarding carbon emissions have driven extensive research aimed at minimizing fossil fuel use and increasing the penetration of renewable and eco-friendly energy sources (RES). To mitigate the devastating effects of climate change, a significant decarbonization of the global economy must be achieved by 2050 [1]. This decarbonization includes transportation electrification (ideally powered by RES) and the implementation of net-zero energy homes and buildings. Furthermore, to enhance resilience, EVs should be capable of supporting homes and buildings during power outages caused by technical faults and extreme weather conditions.

1.3 Net-zero Energy Building

Net zero energy buildings (NZEBs) are ultra-low energy structures that meet their annual energy needs through renewable energy sources, produced either onsite or nearby. The strength of NZEBs lies in their ability to integrate and manage? both the energy supply and demand sides within the same building, optimizing efficiency and sustainability [2]. Key NZEB components are electrical and thermal energy storage units along with an appropriate energy management system.

NZEBs play a crucial role in global energy efficiency strategies. With buildings accounting for approximately 30–40% of the final energy consumption worldwide, reducing their energy demand is essential for achieving a sustainable future [2].

The European Union leads the world in the number of net-zero buildings, driven by government-sponsored retrofit programs and the early adoption of building energy efficiency policies. North America ranks second in this regard [3].

The government of Canada aims to advance NZEBs by developing a "net-zero energy ready" model building code, which provinces and territories are encouraged to adopt by 2030. Additionally, a “model code” (standard) for existing buildings is being developed to guide energy efficiency improvements during renovations, with the goal of adoption across all provinces and territories [4].

Examples of NZEBs across Canada include the Varennes Library, Val-des-Ruisseaux, Experimental House for Building Energetics, and the Future Buildings Laboratory [5]. figure 1-1 illustrates these NZEBs.

Varennes Library, Varennes, Québec [6].

FBL, Loyola Campus, Concordia University [14].

EHBE, Shawinigan, Québec [7]

Figure 1-1: Net-zero Buildings in Canada

1.4 Microgrid and Nano-grid

Microgrids and nano-grids are advanced small-scale power grids equipped with controllable energy sources and storage units. These systems can function either connected to the utility grid or independently in isolation, providing a promising solution to enhance the reliability and resilience of the power sector.

By integrating Distributed Energy Resources (DERs), microgrids and nano-grids can supply active power directly to local loads, thereby reducing transmission and distribution losses. Moreover, they contribute to improved local power quality by offering ancillary services such as voltage support through reactive power injection, assisting in fault restoration with intelligent devices, and maintaining local voltage and frequency control [8].

A nano-grid serves as a fundamental unit within a microgrid. It is designed to operate autonomously, either as part of a cluster or independently in islanded mode. This operational independence significantly enhances the reliability, efficiency, and fault tolerance of the overall smart grid system [8].

1.5 EV integration

To improve the economic justification for EVs while enhancing resilience and power quality, schemes such as vehicle-to-grid (V2G), vehicle-to-home (V2H), and vehicle-to-building (V2B) vehicle-to-load are considered [9]. In these schemes, an EV acts as an electric energy storage element, absorbing and supplying active power based on home or building energy management algorithms. For example, an EV can be charged during low-demand hours (e.g., midnight) and help shave peak demand by delivering electricity to the grid (V2G), home (V2H), or building (V2B) during peak hours [9, 10].

1.5.1 V2G

Plug-in electric and hybrid vehicles, particularly those with larger battery capacities, have the potential to act as backup energy storage for utility grids, addressing the intermittency challenges associated with power grids and renewable energy sources. Consequently, Vehicle-to-Grid (V2G) technology is becoming a vital component of future grid systems. However, these vehicles also need to be charged to meet users' requirements [11], making it essential to develop smart strategies for their charging and discharging when integrated into such grids. Figure 1-2 depicts V2G on top right and V2H on bottom right. [12]

As shown in Figure 1-2, a bidirectional charger is a crucial component for enabling power exchange between an EV and the utility grid. In charging mode, the charger operates in rectifier mode, converting AC to DC to charge the EV battery. Conversely, during V2G operation, it converts DC to AC, enabling the EV to inject power back into the grid.

V2G technologies offer the potential to reduce daily costs for both car owners and utility grid operators by providing the grid with much-needed storage for peak shaving. Through smart grid management, EV charging can be shifted from peak hours to off-peak periods, flattening the daily load curve and reducing the need for additional power generation and infrastructure investment [11].

However, the development of V2G faces several technical, practical, and economic challenges. These include the limited capacity of EV batteries, which could significantly influence the future viability and widespread adoption of V2G systems [11].

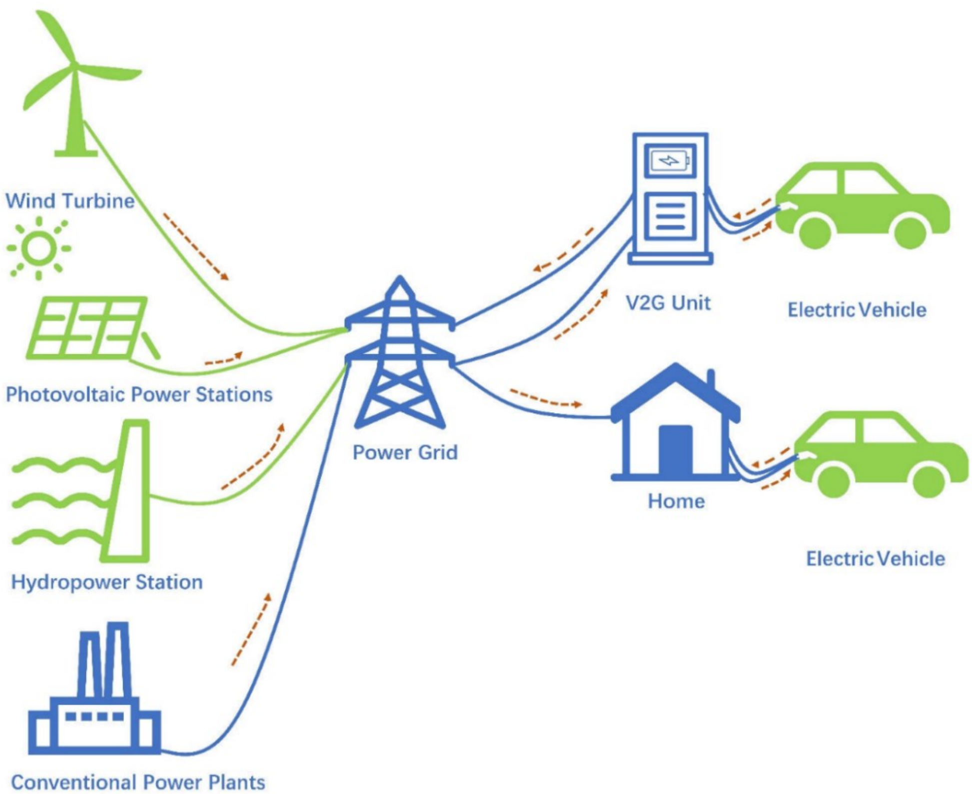

Figure 1-2: V2G and V2H Concept [12]

1.5.2 V2H

Figure 1-2 illustrates the concept of Vehicle-to-Home. In this setup, EVs act as a backup power source during power outages or to help reduce peak electricity demand for household appliances. Similar to V2G, V2H requires a bidirectional interface between the EV and the home [13, 14].

By leveraging the energy storage capabilities of electric vehicles, V2H not only enhances energy resilience but also optimizes energy usage, reduces electricity costs, and supports the integration of renewable energy sources, much like V2G systems [13, 14].

1.5.3 V2L

Another type of EV interface is designed solely for discharging EVs. This type of interface functions as an inverter, converting the DC energy stored in the EV battery into AC power compatible with household appliances. An example is the SETEC 6kW V2L Charger, illustrated in Figure 1-3.

In this research, this EV interface, along with a Nissan Leaf, is utilized as a backup power system for the FBL.

Figure 1-3. SETEC 6kW EV V2L Charger [15]

The integration of EVs with off-grid homes is a growing area of research. For instance, reference [16] explores the use of EVs to support home nano-grids, where the EV functions as a bidirectional storage system. It charges primarily at night using wind energy or when renewable energy production exceeds consumption and discharges during periods when the Hybrid Renewable Energy System (HRES) cannot meet the load demand.

Different interface topologies have been developed to connect EVs and homes. Reference [17] proposes a bidirectional half-bridge DC-DC converter as an interface between an EV and a DC nano-grid with a PV system. In contrast, reference [18] describes an AC-DC converter to link the EV with the Home/Grid, enabling energy support during power outages. Furthermore, integrated onboard power converters with capabilities for Grid-to-Vehicle (G2V), Vehicle-to-Grid (V2G), and Vehicle-to-Home (V2H) functionalities have also been introduced [19].

Recently, commercial bidirectional EV chargers capable of Vehicle-to-Everything (V2X) functionalities have been introduced, although some lack certification for use in North America [20].

1.6 Electrical Vehicles compatible with V2H or V2G technologies

Vehicle-to-Home (V2H) technology allows EVs to supply electricity back to the grid or directly to homes during power outages or peak demand periods. Below are examples of EVs that support or are expected to support V2H technology [14]:

1. Nissan Leaf: Nissan has been a pioneer in V2H technology, and the Nissan Leaf has supported V2H systems in Japan for years. However, availability in other markets may vary. The batteries in the new models are 60kWh with the range of 342km [21]. The model used in this study is Nissan Leaf 2015 with 24kWh battery.

2. Mitsubishi Outlander PHEV: Mitsubishi's plug-in hybrid electric vehicle (PHEV), the Outlander, supports V2H technology in certain markets. The batteries in the new models are 20kWh with the range of 61km [22].

3. Ford F-150 Lightning: The 2022 Ford F-150 Lightning offers V2H for individual owners through its Intelligent Backup Power system. Unlike Nissan Leaf’s V2G focus for fleets, the F-150 Lightning is designed for personal backup power needs. The batteries in the new models are 131kWh with 80A charger [24].

4. Hyundai Ioniq 5 and Kia EV6: These vehicles feature V2L capabilities, providing high-current outlets to power appliances or serve as backup power sources. They are equipped with an Integrated Charging Control Unit (ICCU) capable of supplying up to 3.6 kW of power, suitable for charging devices like electric bikes or camping equipment [23].

V2H is a growing field that offers promising benefits for energy resilience, but its effectiveness depends heavily on the ecosystem in which it operates. These consist of:

Market Availability: V2H technology is not universally available and depends on the region and manufacturer.

Compatible Equipment: V2H systems require compatible charging equipment and local grid infrastructure, which may not be accessible in all areas.

Limitations: Market adoption may also depend on regulatory and utility company support.

1.7 Necessity of Back-up Power

All regions in Canada occasionally experience power outages, often triggered by extreme weather events such as freezing rain, hailstorms, geomagnetic storms, or high winds, which can damage power lines and equipment. Wildfires, increasingly frequent due to climate change, also pose a significant threat to the electrical supply network. Additionally, during heat waves and cold snap, the power system can become overloaded, leading to outages [24].

Power outages can significantly affect both your health and your property. Extended outages may lead to frozen water pipes, communication disruptions, limited access to essential goods, food and water contamination, and health risks from exposure to extreme heat or cold. Additionally, improper use of generators during outages can result in carbon monoxide poisoning [24].

Figure 1-4 shows the reported power outages by region in Canada from 2011 to 2017. The data clearly indicates an upward trend in the number of power outages during this period.

In today's technologically advanced and interconnected world, the need for emergency backup power is more critical than ever. Unexpected events such as severe weather, natural disasters, or equipment failures can lead to widespread power outages, disrupting essential services and posing significant risks to public safety, health, and economic stability [14].

Emergency backup power systems enable critical facilities (such as hospitals, data centers, communication networks, and emergency response centers) to maintain essential operations during crises. These systems ensure the functionality of life-saving equipment, the protection of vital data, and the continuity of crucial communication channels. Moreover, backup power systems can mitigate the impact of prolonged power outages on homes and businesses, providing communities with a sense of security and preparedness in the face of challenging conditions [14].

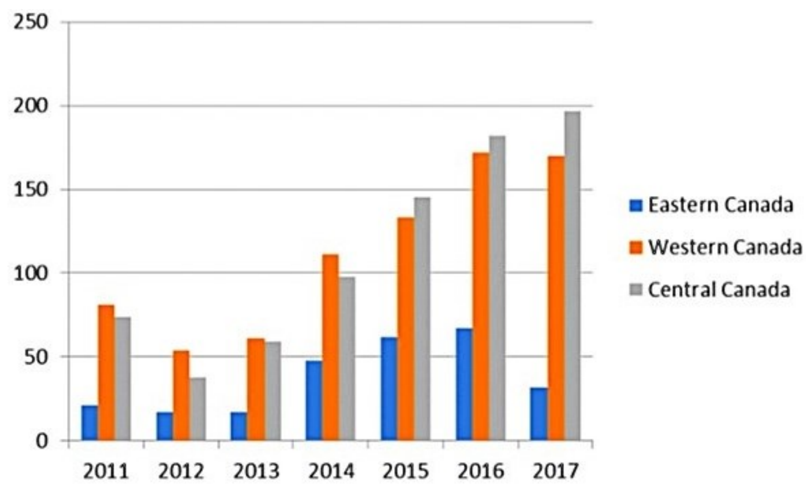

East: Newfoundland, New Brunswick, Nova Scotia, Prince Edward Island

West: Alberta, British Columbia, Manitoba, Northwest Territories, Saskatchewan, Yukon

Central: Ontario, Quebec

Figure 1-4. Reported power outages by region in Canada [25]

1.8 Backup Power technologies

There are several backup power technologies available to ensure a reliable supply of electricity during power outages, including the following:

Standby Generators:

Electric power generators are a widely used source of emergency power. Their engines can be powered by bottled or natural gas, gasoline, or diesel. The generator is connected to the load and the normal power supply via a transfer switch [26].

Under normal conditions, the transfer switch connects the load to the utility power source. In the event of a utility power outage, the generator starts, and the transfer switch shifts the load to the generator. This process typically takes about 10 seconds. Once utility power is restored, the transfer switch reconnects the load to the utility power source after a delay of approximately 15 minutes to ensure stability [26].

Uninterruptible Power Supply (UPS):

A battery-powered Uninterruptible Power Supply (UPS) provides immediate, short-term alternative power using batteries. There are two primary techniques for battery-powered UPS systems:

Line-Interactive UPS: In this configuration, a switch transfers the load from the utility grid to the backup inverter during an outage. The transfer process takes a few milliseconds depending on the speed of internal transfer switch, ensuring minimal disruption.

Double-Conversion UPS: This system uses two back-to-back converters with a storage battery connected to the central DC bus. In this design, the transition from utility grid power to backup battery power is instantaneous, providing seamless power delivery without interruption.

Renewable Energy Systems with Storage:

Wind and solar resources and technologies complement each other, enhancing the reliability of a power system while being more cost-effective when integrated. Critical components such as batteries and inverters play a key role in enabling hybrid systems to store and distribute energy efficiently [26].

Fuel Cells:

A fuel cell operates similarly to a battery, generating power through chemical reactions. It is a device in which hydrogen and oxygen react in a controlled manner to produce water, heat, and a flow of electrons, which creates electricity via an external circuit [26].

Currently, most fuel cell systems are used in commercial applications and operate on a "reformate" derived from natural gas. However, the widespread availability of hydrogen would enable the use of direct hydrogen fuel cells. These systems are simpler, more cost-effective, and offer greater reliability compared to those relying on reformate [26].

Vehicle-to-Grid (V2G) and Vehicle-to-Home (V2H)

An EV used as a UPS system differs significantly from traditional UPS systems because it is mobile, meaning its battery may not always be fully charged in the event of a power outage. Additionally, the EV cannot charge or discharge itself while traveling and not plugged in at home. When the EV is plugged in and the grid is functioning normally, it can charge itself using the bi-directional DC/AC converter. In the event of a grid failure, the EV discharges power to supply the load [27].

Using an EV as a Backup Power Source has its advantages and disadvantages. Being eco-friendly and cost-effective are advantages of such a concept. This means EVs generate zero emissions when supplying backup power, making them an environmentally friendly option. In addition, EV owners, using the vehicle as a backup power source do not need to purchase a separate generator or backup power system, reducing costs [14, 28].

There are some drawbacks for this concept such as limited battery capacity and battery degradation. This means an EV's battery capacity may not be sufficient to power an entire home for a prolonged period, particularly if the vehicle is also required for driving during the outage [29]. Frequent use of an EV's battery for backup power also can accelerate battery wear and reduce its overall lifespan over time [14, 28].

By weighing these advantages and limitations, users can better understand how to integrate an EV into their energy resilience strategies effectively.

Flywheel Energy Storage

Flywheel systems store kinetic energy in a rotating mass, typically a high-speed spinning disk. This energy can be converted back into electrical energy when required, providing a reliable and efficient backup power source [30]. Flywheels are often used in applications that require rapid bursts of energy or short-term power support, as they can quickly release stored energy, and this energy cannot last long.

Each of these options has its advantages and disadvantages. Therefore, it is essential to consider factors such as cost, availability, efficiency, and environmental impact when selecting a backup power solution.

1.9 Focus and Objectives

This work focuses on integrating an EV into a three-phase PV + battery SMA system using a low-cost single-phase Vehicle-to-Load (V2L) inverter. Although this inverter communicates with the EV Battery Energy Management System (BEMS), it is designed to supply an isolated load and cannot operate in parallel with other sources or storage units. The primary objective is to enhance system resilience by utilizing the EV as a secondary energy storage system. Additionally, the work introduces an energy management strategy for operation during utility power outages, incorporating load shedding based on the SoC of the stationary battery.

The setup utilizes SMA Sunny Boy (SB) inverters for PV generation and Sunny Island (SI) inverters for battery management, with a Data Manager (DM) for system monitoring and control. Additionally, the system includes an EV that can be charged using a standard 208V unidirectional charger during grid-connected operation.

To enable the EV to support the nano-grid, the V2L inverter is connected through a fourth Sunny Island inverter (SI4), allowing the EV to charge the stationary battery. An energy management strategy has been devised to extend load supply after transitioning from grid-connected mode to islanded mode. This strategy includes:

EV Battery Support: Leveraging the EV battery to supplement the stationary battery during critical conditions.

Load Shedding: Implementing a scheme to prioritize essential loads and manage the SoC of the stationary battery effectively.

Experimental results validate the feasibility of the proposed energy management scheme, demonstrating its effectiveness in maintaining reliable power supply and optimizing the use of available resources.

1.10 Test Environment and Methodology

The proposed system is tested at the Future Building Laboratory (FBL), which employs SMA products. While commercial equipment offers reliability, it often lacks flexibility to prevent non-expert users from configuring potentially unsafe systems. Therefore, the methodology developed in this work is designed to align with the features and constraints of commercial equipment. It is noteworthy that SMA offers products like the SMA Home Manager 2, which provides advanced home management features, including weather forecasting and communication with smart devices. However, this product is unavailable in North America, necessitating alternative approaches.

The FBL (Figure 1-1), which is in Loyola Campus, is a research facility for buildings of the Future. The exact location of the house is shown in Figure 1-5.

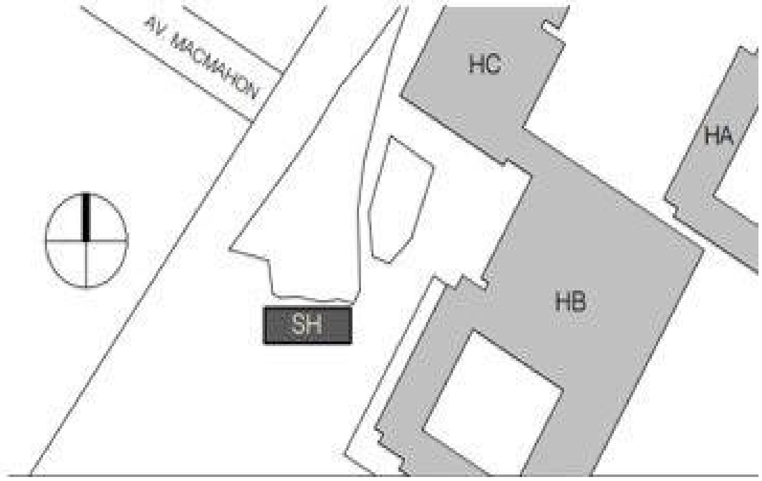

Figure 1-5: Location of the FBL in Loyola Campus shown as SH building in the map [14].

1.11 Resilience

Resilience in electrical power systems refers to the system's ability to anticipate, absorb, adapt to, and rapidly recover from disruptive events [31]. The SMA system demonstrates several resilience features, notably the islanding capability of the SMA SI inverter. This function enables the SI to maintain power supply to isolated (islanded) sections of the grid, ensuring that critical loads remain operational during power outages or abnormal utility grid conditions. Moreover, the system can adapt to rapid fluctuations in load conditions, a particularly valuable feature when operating on weak or unstable buses. Additionally, the system incorporates an energy storage component (a stationary battery), which facilitates a fast load demand response and contributes to system stabilization under stress.

In this study, the integration of an electric vehicle (EV) battery into the FBL nanogrid extends the duration of critical load support and photovoltaic (PV) generation beyond the limitations of the stationary battery. The proposed scheme also incorporates load shedding, which involves disconnecting lower-priority loads to prolong the supply to higher-priority ones. Both load shedding and the inclusion of the EV battery effectively increase the overall energy capacity and operational duration of the SMA system—in other words, they extend the period during which the SI inverters remain active—thereby enabling greater utilization of PV generation. Collectively, the

EV battery, load shedding, and PV generation enhance the resilience of the proposed system by improving its ability to absorb the impacts of power disruptions and adapt to outage conditions. While the system is not capable of anticipating power disruptions, it demonstrates self-recovery following the restoration of normal utility grid conditions by recharging the stationary battery and restoring previously shed loads. This behavior is further discussed in 5.85.8.

Measuring resilience is inherently complex, as it encompasses multiple dimensions and dynamic factors. Nevertheless, quantifying resilience is crucial for evaluating the effectiveness of resilience strategies and for making necessary adjustments. Although numerous resilience metrics have been developed, they often capture only a limited subset of the overall resilience framework. These metrics typically focus on specific aspects, such as a system’s robustness to initial disturbances, the level of functionality maintained during a disruptive event, or the time required for post-event recovery [32]. In this context, Reference [32] employs Equation 1-1 to define a resilience index.

$$R = \frac{\int_{t_0}^{t_1} Q(t)dt}{(t_1 - t_0)} \qquad \text{1-1}$$

In this research, the primary objective is to enhance the functionality of the islanded grid. Accordingly, resilience is defined in terms of the functionality maintained by the FBL loads supplied by the SMA system during a power outage.

In this study, a normalized resilience index is employed, as defined in Equation 1-2. In this formulation, a value of R=1 indicates that the system remains fully functional throughout the time interval from t_0 to t_1, while R=0 signifies a complete loss of functionality during the same period. The use of a normalized resilience index is justified by the varying durations of different operating conditions—namely, normal operation, islanding, and load shedding—allowing for a consistent and comparative evaluation of system performance across these scenarios.

$$R = \frac{\int_{t_0}^{t_1} Q(t)dt}{Q(\infty) * (t_1 - t_0)} \qquad \text{1-2}$$

R: normalized resiliency index

Q (∞): Capacity of fully functional system

Q (t): Functional capacity of the system at "t"

This would be discussed in detail in result chapter.

1.12 Contribution

The contribution of this thesis lies in the integration of an EV equipped with a low-cost, single-phase V2L inverter (designed to support isolated loads) into a three-phase PV + battery-powered system based on commercial SMA inverters. This work is particularly innovative because the V2L inverter, unlike grid-following inverters, cannot directly connect to the grid or to the three-phase SMA inverters (Sunny Islands), as the SMA system detects single-phase inverters as faulty. The proposed method, however, successfully overcomes these limitations, making this integration viable.

The most significant advantage of the proposed method is that it establishes a foundation for use in future research. While the current test setup is designed to extend the feeding time of priority loads (effectively functioning as V2H), it can also be adapted for V2G applications. Additionally, the research demonstrates that DC sources, such as fuel cells or DC wind turbines, can be connected to the DC bus of the stationary battery, further broadening the potential applications of the system.

1.13 Thesis Structure

This thesis is organized as follows:

Chapter 2: This chapter offers a comprehensive analysis of the FBL, including building's electrical infrastructure and the characteristics of the loads connected to the system.

Chapter 3: This chapter provides a detailed outline of the specifications for the components used in the test system at the FBL. These components include the PV arrays, PV inverters, battery bank, battery inverters, SMA Data Manager M, ioLogik E1242, EV, and SETEC V2L inverter.

Chapter 4: This chapter will examine the electrical and data connections of the components discussed in Chapter 3. It will also address the limitations encountered during the preparation and execution of the test setup, followed by a detailed explanation of the corresponding solutions implemented to overcome these challenges.

Chapter 5: This chapter will cover the proposed procedure for utilizing the EV battery to support the AC nano-grid during critical utility outage conditions, as well as the energy management strategy employed to achieve this objective.

Chapter 6: This chapter presents the practical test results obtained from running the test setup with the implemented energy management strategy, validating the effectiveness of the proposed approach.

Chapter 7: This chapter concludes the thesis and offers suggestions for future work.

Chapter 2 - Future Buildings Laboratory

2.1 Introduction

This chapter provides detailed specifications of the Future Buildings Lab site, including its electrical infrastructure and the characteristics of the connected loads.

2.2 Building Specifications

The FBL features a ground floor area of 103 m², comprising six cells (four of which are test cells), an electrical room, a mechanical room, and a 24 m² mezzanine. Figures 2-1 and 2-2 illustrate the layouts of the ground floor and mezzanine, respectively.

The building incorporates Building Integrated Photovoltaics (BIPV) in one test cell and Semi-Transparent Photovoltaics (STPV) in the other three test cells. Additionally, the roof is equipped with three racks designed for the future installation of PV panels.

The FBL also supports advanced energy technologies, including EVs, fuel cells, and wind turbines, making it a versatile platform for renewable energy research and testing.

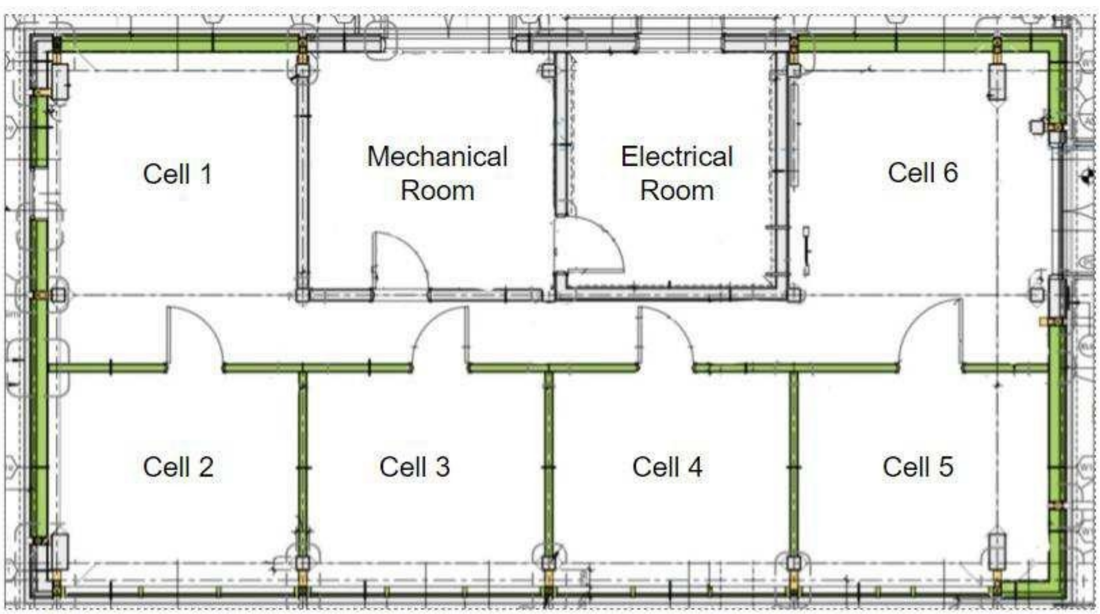

Figure 2-1: Map of the ground floor [14].

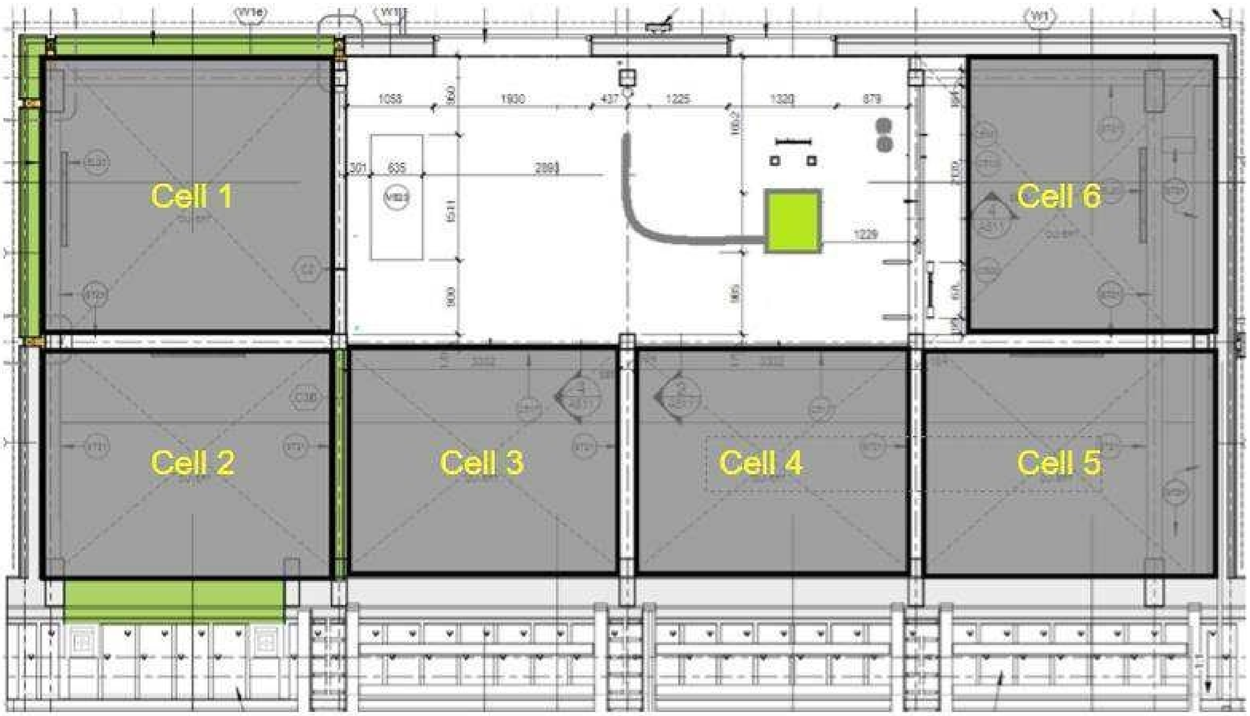

Figure 2-2: Map of the mezzanine [14].

2.3 House Load

As discussed, the aim of this thesis is to utilize the EV battery along with the stationary battery during emergencies or power outages to provide sufficient backup power for supporting priority loads. In other words, the goal is to extend the duration for which priority loads can be sustained.

To achieve this, it is essential to have a comprehensive understanding of the loads at the FBL. The very first list of loads at the FBL is listed in Table 2-1.

Table 2-1: The First Plan for Main Panel at FBL[1]

Sign:	**P1-110.01- SH**					**Location: In origin of:**	T1-210.00- SH			**Volts:**	120/208	**Phases:**	3
Circ.	**Description of circuit**	**C.B.**	**P.**	**A**		**B**		**C**		**P.**	**C.B.**	**Description of circuit**	**Circ.**
1	LIGHTING OUTSIDE	15 A	1	105 VA	826 VA					1	15 A	LIGHTING MEZZANINE AND WELL LUM	2
3	LIGHTING GROUND FLOOR	15 A	1			891 VA	1424 VA			1	15 A	LIGHTING GROUND FLOOR	4
5	SOCKET OFFICE IT	20 A	1					120 VA	120 VA	1	20 A	SOCKET	6
7	SOCKET OFFICE IT	20 A	1	120 VA	2000 VA					2	20 A	SOCKET	8
9	SOCKET(S) ROOM ELEC/MEC	15 A	1			240 VA	2000 VA						10
11	COUNTER	15 A	1					0 VA	120 VA	1	20 A	SOCKET	12
13	AEROHEAT	15 A	2	750 VA	2000 VA					2	20 A	SOCKET	14
15						750 VA	2000 VA						16
17	HU1-001-110.00- SH	30 A	2					2025 VA	500 VA	1	15 A	HOUSING ALARM INTRUSION DSC	18
19				2025 VA	120 VA					1	20 A	SOCKET	20
21	CE1-ECD-110.00- SH	20 A	2			1500 VA	2000 VA			2	20 A	SOCKET	22
23								1500 VA	2000 VA				24
25	AEROHEAT	15 A	2	750 VA	120 VA					1	20 A	SOCKET	26
27						750 VA	2000 VA			2	20 A	SOCKET	28
29	VE1-002-110.01- SH	15 A	1					75 VA	2000 VA				30
31	Free	50 A	2	0 VA	120 VA					1	20 A	SOCKET	32
33						0 VA	2000 VA			2	20 A	SOCKET	34
35	EC1-002-110.01- SH	15 A	1					500 VA	2000 VA				36
37	CC1-R410a.001-EXT- SH	45 A	2	3700 VA	120 VA					1	20 A	SOCKET	38
39						3700 VA	2000 VA			2	20 A	SOCKET	40
41	TERMINAL OF RECHARGE	40 A	2					500 VA	2000 VA				42
43				500 VA	7500 VA					2	100 A	SE1-001-210- SH	44
45	CONNECTION FUTURE (BOILER)	30 A	3			2333 VA	7500 VA						46
47								2333 VA	120 VA	1	15 A	SOCKET	48
49				2333 VA	65 VA					1	15 A	CONNECTION FUTURE (PUMP)	50
51	SIGN OF COMMUNICATION WITH...	15 A	1			500 VA	100 VA			1	15 A	DOOR ELECTRIFIED	52
53	SIGN ALARM CONTROL FIRE	15 A	1					500 VA	100 VA	1	15 A	SIGN ISTAR	54
55	Free	20 A	1	0 VA	0 VA					1	20 A	Free	56
57		- -	- -			0 VA	0 VA			- -	- -		58
59		- -	- -					0 VA	0 VA	- -	- -		60
61		- -	- -	0 VA	0 VA					- -	- -		62
63		- -	- -			0 VA	0 VA			- -	- -		64
65		- -	- -					0 VA	0 VA	- -	- -		66
67		- -	- -	0 VA	0 VA					- -	- -		68
69		- -	- -			0 VA	0 VA			- -	- -		70
71		- -	- -					0 VA	0 VA	- -	- -		72
			Total Power :	23154 VA		31688 VA		16439 VA					
	Total Connected Power :			202 A		273 A		137 A					
				71281 VA				**Bus bars :**				**400 A**	

[1] This table is the translation of FBL documents

Note: A socket refers to any type of outlet, such as a plug. A load, such as a microwave, can be connected to it. In some cases, the socket may be free and not in use.

As shown in the "Total" row of Table 2-1, the total power for each phase (Phase A, B, and C) exceeds the maximum continuous power rating of the SMA inverters (5,750 W each). This indicates that not all loads at the FBL can be connected to the SMA system, in case of power outages. Therefore, only a portion of the FBL loads can be supported by the SMA system, and these are designated as "Priority Loads". The remaining loads are categorized as "Non-Priority Loads".

Since these two groups of loads are powered by different sources, they are housed in separate panels. Non-Priority Loads are powered by the transformer and connected to the main panel while Priority Loads are powered by the SMA system and connected to the sub-panel.

Note: Even under normal utility grid conditions, when the SIs connect the utility grid to the load side via isolation relays, the load demand is still supplied through the SIs rather than directly from the grid. Therefore, these priority loads should be accommodated in a dedicated sub-panel.

The utility grid/generator side of the SMA system is connected to the main panel through a 50A 3-phase circuit breaker. The circuit diagram of the electrical system at the FBL is illustrated in Figure 2-3.

Note: to allow the priority loads to be fed directly from the utility grid, bypassing the SMA system, a transfer switch (TS1) has been added to the system. By switching TS1 to the utility grid position, the input of the sub-panel will be directly connected to the main panel, bypassing SMA system.

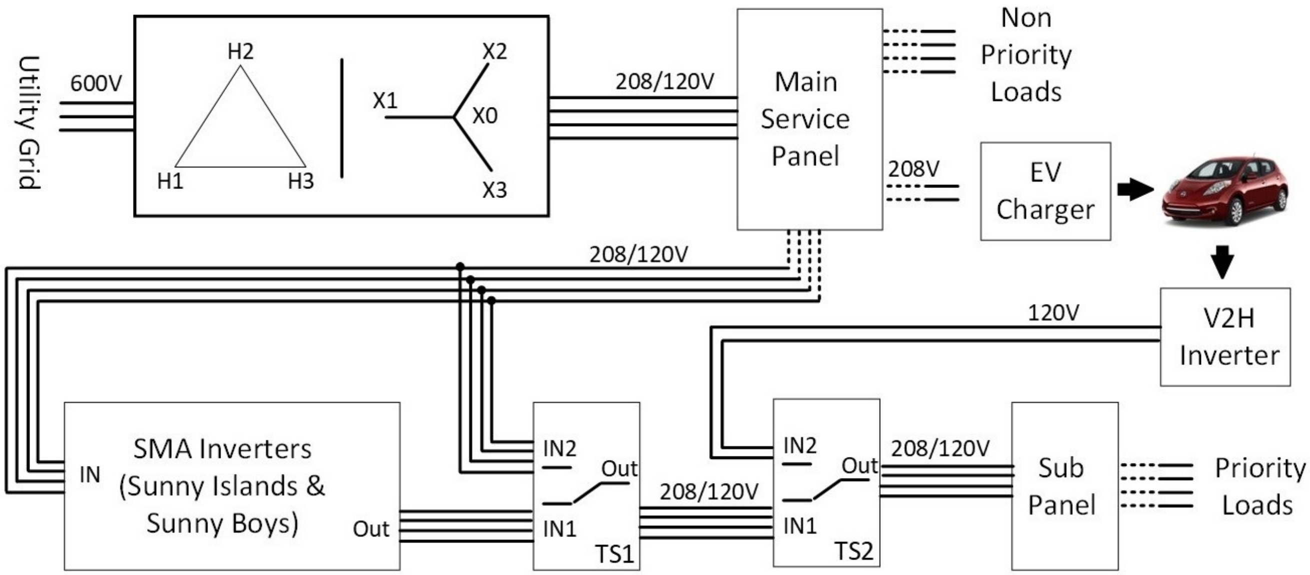

Figure 2-3: Electrical connections at FBL

Note: Figure 2-3 illustrates the current/permanent electrical configuration at the FBL. In this setup, the EV can be connected as a V2L system, allowing a single-phase V2L inverter to supply single-phase loads. This can be done by changing the position of transfer switch 2 (TS2) shown in figure 2-3.

However, to implement the proposed connection that enables the single-phase V2L inverter to contribute to feeding 3-phase loads, certain modifications are required. These modifications are discussed in detail in Chapter 4.

As discussed above, a portion of the loads must be transferred to/accommodated in the Sub-Panel. Table 2-2 lists these loads, including their ratings and the phases to which they are connected.

Table 2-2: Priority Loads at FBL

No	Load	Phase A (VA)	Phase B (VA)	Phase C (VA)
1	EXTERIOR LIGHTING	105		
2	MEZZANINE LIGHTING AND LIGHT PIT	826		
3	GROUND FLOOR LIGHTING (CIR.3)			891
4	GROUND FLOOR LIGHTING (CIR. 4)			1424
5	Heater (CIR. 13)	750		
6	Heater (CIR. 14)		750	
7	Humidifier (CIR.17)		2025	
8	Humidifier (CIR.19)	2025		
9	DCS Intrusion Alarm Box (CIR.18)			500
10	Greenheck Fan (CIR.29)			75
11	Air Exchanger (CIR. 35)			500
12	COMMUNICATION PANEL (CIR.51)			500
13	FIRE ALARM CONTROL PANEL			500
14	ISTAR PANEL (Door Controller)			100
Total		3706	2775	4490

As shown in the Total row of Table 2-2, the loads are distributed across all three phases.

Note: FBL is a laboratory where students from other departments, such as Building and Chemical Engineering, conduct tests. These experiments may need to run continuously for extended periods, sometimes spanning several months. To avoid interference with ongoing projects, the work conducted in this thesis does not use the actual building loads. Instead, three controllable loads and a three-phase dump load are utilized as priority loads.

Chapter 3 - Main System Components

3.1 Introduction

This chapter outlines the specifications of the components used in the test system at FBL. These components consist of PV arrays, PV inverters, battery bank, battery inverters, SMA Data manager M, ioLogik E1242, EV, and SETEC V2L inverter.

3.2 PV arrays

As Figure 3-1 illustrates, 12 solar terra Copper 210Wp, 12 Grey 210Wp and 12 Black 230Wp arrays are in the process of being installed on the rooftop of FBL. The arrays' rated powers are of 2520, 2520 and 2760 Wp, respectively. The last one will be used as BIPV/T for electricity generation and heat recovery.

Figure 3-1:Solar arrays on the roof of the FBL [14].

3.3 PV inverters

Three SMA SBs (Sunny Boy 7.0-US) convert the DC power produced by the rooftop PV arrays into AC and deliver it to the nano-grid. This model, in single-phase/split-phase mode is capable of supporting 120V, 120/208V, 208V, or 240V and in three-phase mode, 208 or 240 V_{LL}. Its maximum DC input voltage is 600V. Its Maximum Power Point Tracking (MPPT) voltage range is 100-550V with an initial voltage of 125V. Its rated power at 240V AC is 7 kW and at 208V AC it is 6650W. It has a maximum efficiency of 97.9% at 240V. It has 3 MPPT inputs [34]. The 3 Sunny Boys installed at FBL are shown in figure 3-2.

Figure 3-2: PV inverters (Sunny Boy 1, 2, and 3) at FBL.

3.4 Battery bank

The battery bank of this system (shown in figure 3-3) consists of 6 units of Pylontech - US3000C, forming a 21.3 kWh bank with nominal voltage of 48V. This battery is of the LiFePO4 type, and each unit has a nominal capacity of 3.55 kWh with 3.37 kWh of it being usable. The lifetime of this battery would be 6000 cycles in Depth of Discharge (DOD) of 95%. The top battery unit is the master, and the five others are slaves. The slave battery units communicate with the master one through link port terminals and wired in chain configuration. The master SI unit communicates with the master battery unit through a CAN and transfers battery information to the DM through RS485 [35].

Figure 3-3: 6 units of Pylontech - US3000C connected in parallel

3.5 Battery Inverters

Three SMA SIs (Sunny Island 6048-US) are used in the FBL system. Their nominal battery voltage is 48 V (41-63 V), the rated power is 5750W, and the maximum efficiency is 94 %. The nominal AC voltage is 120 V (105-132 V), with them being connected in star. The nominal battery charging current is 110 A with a maximum of 130 A. This charging current is adjustable. The AC side current is also adjustable: 0-56 A. It accepts Lead-Acid, NiCd and Li-ion batteries from 100 Ah to 10000 Ah [36]. The Sunny Islands installed at FBL are shown in figure 3-4.

Figure 3-4: Battery inverters (Sunny Island 1, 2, and 3)

Figure 3-5 shows the internal connections of an SI. The battery bank is interfaced to load/SB through a “bidirectional inverter” which balances PV generation and load demand when forming the grid in the islanded mode. The utility grid/generator terminal is connected to the load/SB terminal through an isolating relay. In case of power outage or deviation of utility grid/Generator voltage and/or frequency out of predefined range, the SI opens the internal isolation relay. When the grid/generator resumes with the required parameters, the “bidirectional” inverter resynchronizes to the grid/generator, the SI closes the internal isolation relay, and the “bidirectional inverter” returns to the grid-following mode [36].

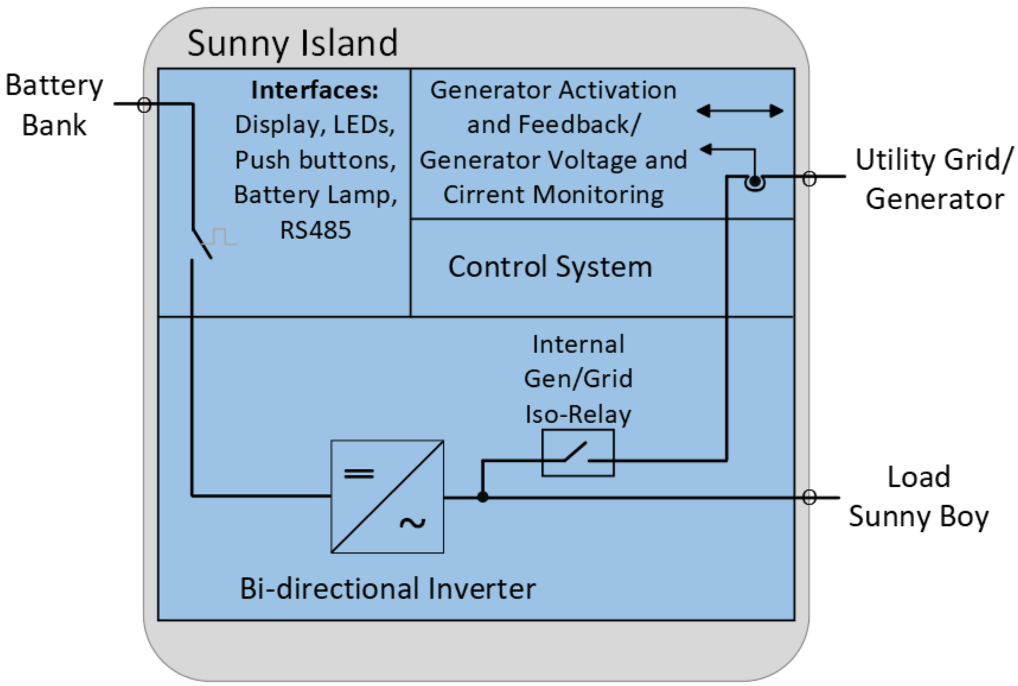

Figure 3-5: Internal connection of Sunny Island inverter [37]

3.6 SMA Data Manager M

The Data Manager M (figure 3-6), in combination with the Sunny Portal powered by ennexOS, enables effective monitoring, management, and grid-compliant power control for decentralized PV systems. It supports up to 50 devices with an inverter capacity of 2.5 MVA in closed-loop control mode, or up to 7.5 MVA in open-loop control or monitoring mode. With the help of the user interface of ennexOS, it is possible to monitor the instantaneous and accumulated values of system variables such as PV generated power or battery SoC. It is also possible to perform grid and energy management strategies ranging from load shedding to active and reactive power control of the system [40].

Figure 3-6: SMA Data Manager M [34]

3.7 ioLogik E1242

The I/O device used in this project is the ioLogik E1242. It is equipped with 4 analog inputs, 4 digital inputs, and 4 digital configurable digital inputs/outputs. It also has a 2-port Ethernet switch for daisy-chain connections [39]. Figure 3-7 the ioLogik E1242.

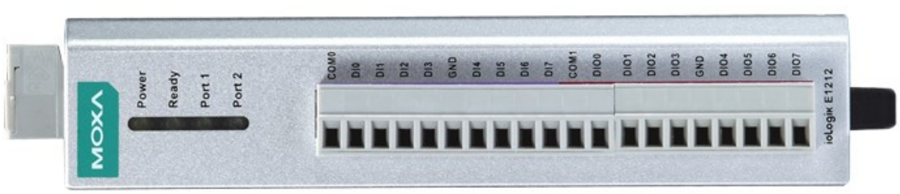

Figure 3-7: ioLogik E1242 [39]

3.8 Vehicle to Home Inverter (SETEC)

For using the EV to support critical loads of the FBL a single-phase V2L SETEC Power inverter shown in Fig. 3-8 is employed. It is rated at 6 kVA, 110 V/ 60 Hz. It is intended to supply isolated loads with regulated voltage and frequency. It communicates with the BMS of the EV and keeps supplying the load as long as the SoC of the battery is above 30%. It is also protected against overload and short circuits in the AC side. However, it is unable to operate in parallel with other power units, grid or inverters [40]. One option to benefit from the energy stored in the EV to support the three-phase system, is to connect the EV to the stationary battery. For that, one can employ a simple 48 V battery charger in series with the single-phase SETEC V2L inverter. The problem is that these usually do not provide much flexibility to control the power flow from the EV, V2L inverter, to the stationary battery, which should only occur when the latter is at critical SOC. That is why a fourth SI is used in this work. This will be discussed in detail in chapter 4.

Figure 3-8: 6kVA SETEC Power Vehicle-to-Load (V2L) Inverter [40]

3.9 Electric Vehicle

A Nissan leaf model 2015 with a 400 V, 24 kWh Lithium-ion battery bank is included in the FBL system. Its original portable charging cable works with 100-120 V/15 A or 200-250 V/ 20 A [41]. The charger used at the FBL is a 208V Grizzl-E mini level 1-2 EV charger, delivering up to 40 A [42]. Figure3-9 shows Nissan Leaf connected to SETEC V2L inverter, V2L inverter connected to its point of connection to FBL, and the black box which is Grizzl-E mini level 1-2 EV charger.

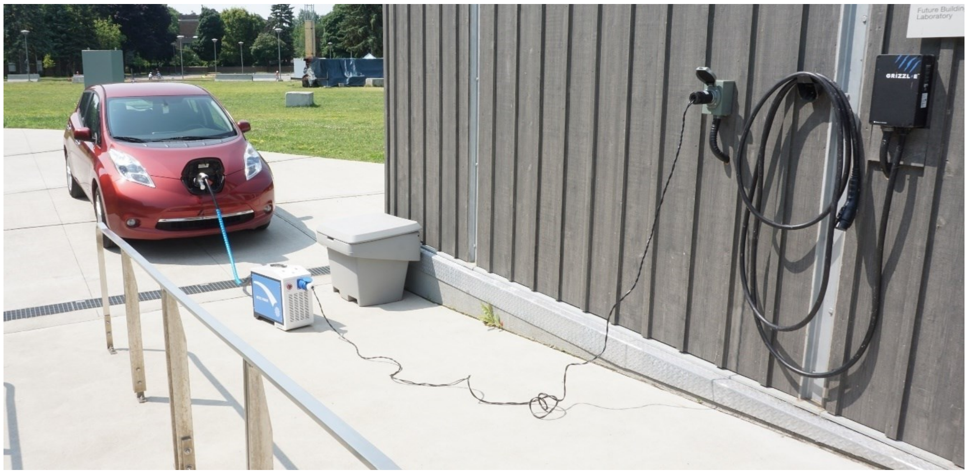

Figure 3-9: Nissan Leaf, Grizzl-E mini level 1-2 EV charger, and V2H Connection terminal

3.10 Transformer

The transformer used at the FBL is a 150 kVA step-down transformer with a primary winding of 600V delta and a secondary winding of 208Y/120V star. Figure 3-10 shows the nameplate of the installed distribution transformer at the FBL.

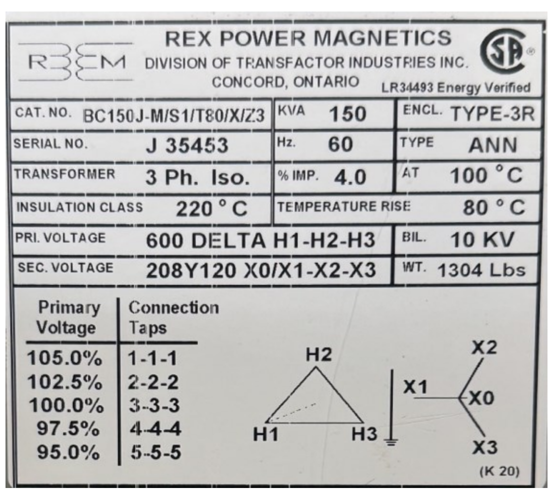

Figure 3-10: Installed distribution transformer at FBL

3.11 Main-Panel

The main panel (shown in figure3.10) is Square D, 400 Amp 72-Space Main Lug 3-Phase 120/208Y V. The main panel is fed from the transformer and all loads including SMA system and EV charger are fed through breakers in this panel.

Figure 3-11: Main Panel

3.12 Sub-Panel

The sub-panel is Siemens ES Series 125 Amp 12-Space 24-Circuit Main Lug 3-Phase 120/208Y V. It is shown in figure 3-11. The sub-panel is fed from SMA system and priority loads (level 1 and 2) are fed through breakers in this panel.

Figure 3-12: Sub-Panel

3.13 Controllable Loads

Chroma 63802 is a programmable AC/DC electronic load with 1800W peak power. The supply voltage for the controllable load is 110/240V, while the test bench voltage varies from 50 to 350Vrms. The current range is 0-18Arms, with the peak current and voltage being 54A and 500V respectively. This load can work in Constant Current (CC) mode, Constant Resistance (CR) mode, Constant Power (CP) mode, and Rectified load mode. In CC mode, the programmable current range is 0-18Arms, with 2mA resolution, and 0.1%+0.2% full scale accuracy. In CR mode, the resistance range is 2.77Ω-2.5KΩ, with 20µΩ resolution, and 0.5%+0.5%F.S. accuracy. In CP mode, the power range is 0-1800W, with the resolution of 0.375W and 0.5%+0.5%F.S. accuracy. In CC and CP mode the range of crest factor is 1.414-5.0, with the resolution of .005. Power Factor range is 0-1 Lag/Lead, with 0.001 resolution. In DC section, voltage range is 7.5-500V, current range is 0-18A, with the rase time of 75µs [43]. As it is shown in figure 3-12, constant resistor mode is used with R=12.3Ω, consuming 1141.68W in the grid voltage of 118.53V. In this work, three chroma controllable loads are used as a 3-phase controllable load.

Figure 3-13: Chroma Controllable Load

Chapter 4 - Experimental Setup

4.1 Introduction

The previous chapter outlined the main components used in this work. This chapter will consider their electrical and data connections. Certain limitations were encountered during the preparation of the test setup and the execution of the test. Following the discussion of the experimental setup, these limitations and their corresponding solutions are outlined in detail.

The proposed test setup diagram is shown in figure 4-1.

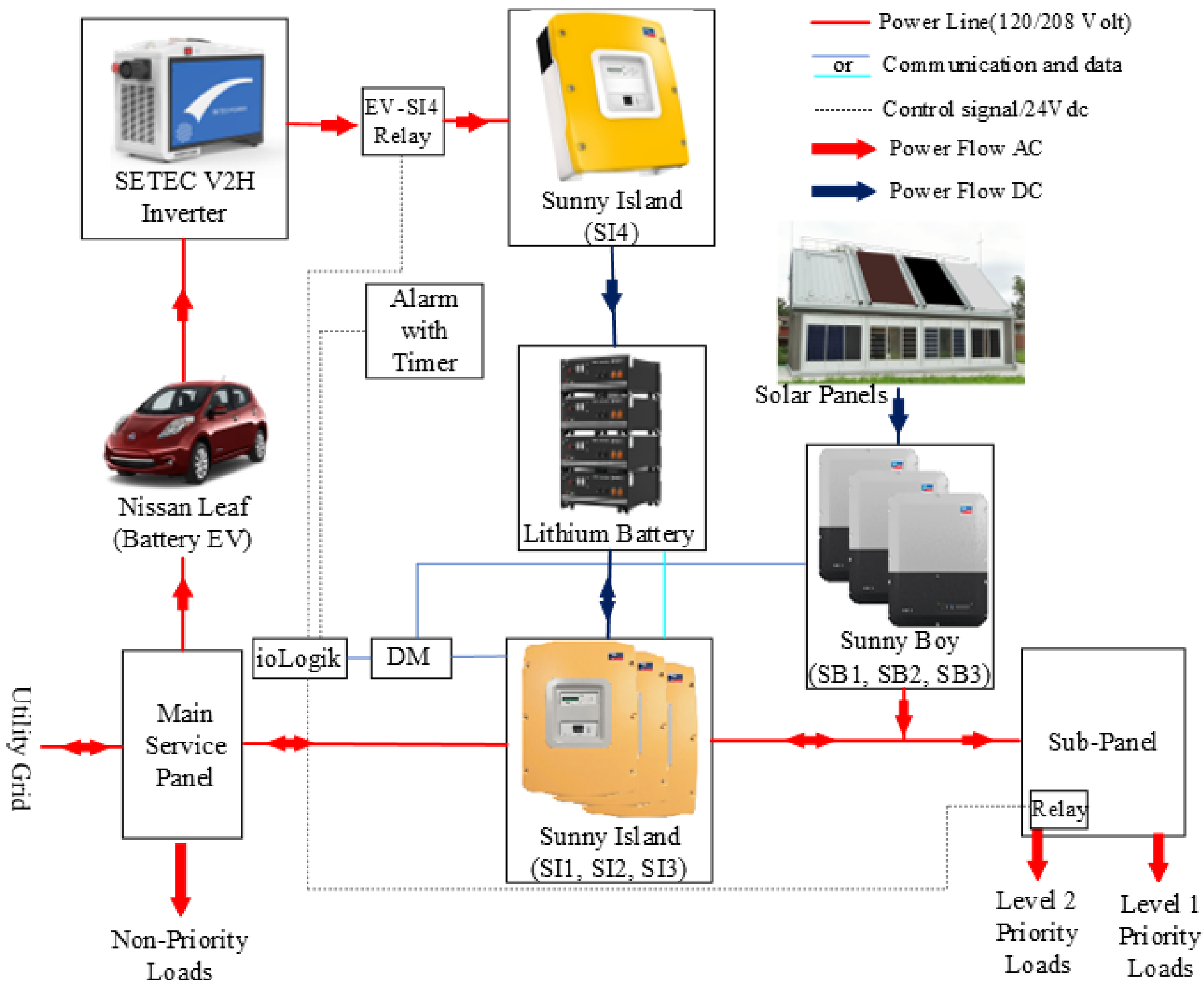

Figure 4-1: Chroma Controllable Load

This setup can be divided into the following five sub-parts:

1- Load Centers (Main Panel + Sub-panel)
2- PV Powered Unit (Rooftop PVs + Sunny Boy Inverters)
3- Battery Powered Unit (Sunny Island Inverters + Stationary Battery)
4- Backup Unit (EV + SETEC Inverter + SI4)
5- Data and control Unit (Data Manager + ioLogik E1242 + EV-SI4 relay + Load Shedding Relays + Alarm)

4.2 Load Centers

The loads at FBL are categorized into two types: “Priority Loads” and “Non-Priority Loads”. As shown in Figure 4-1, the Non-Priority Loads are connected to the main panel, while the Priority Loads are supplied through the sub-panel. This separation into two load centers is necessary because of their different power sources: Non-Priority Loads are powered by the transformer, whereas Priority Loads are mainly supplied by the SMA system.

Note: Even when the utility grid is normal, SIs link utility grid to priority loads via isolating relays, this energy pass through SIs and priority loads find SIs as their source of power.

The EV charger outlet and the SMA system are powered from the main panel via 40A two-phase and 50A three-phase breakers, respectively.

4.3 PV Powered Unit

Figure 4-2 presents the schematic diagram of the proposed PV and battery system. On the right side of the figure, the PV system is depicted, comprising PV arrays and three SB units. Each PV array is connected to the MPPT terminal C of its respective SB via a fusible disconnect switch to ensure safety.

Although the SBs can be configured in a Delta arrangement, they are connected in a Star configuration in this test setup. This design ensures that each SB corresponds exclusively to one SI. Consequently, if one SI experiences a failure, only the associated SB ceases power generation, preserving the operation of the other SBs.

In contrast, in a Delta configuration, each SB (208V) is connected to two phases, effectively making it dependent on two SIs for operation. In this arrangement, a failure in any one SI would result in two SBs losing the ability to generate PV power.

Therefore, the Star configuration significantly enhances the system's resilience and reliability by limiting the impact of SI failures. In the event of an SI malfunction, the PV power output in the Star configuration is higher than in the Delta configuration, optimizing overall system performance and minimizing disruptions.

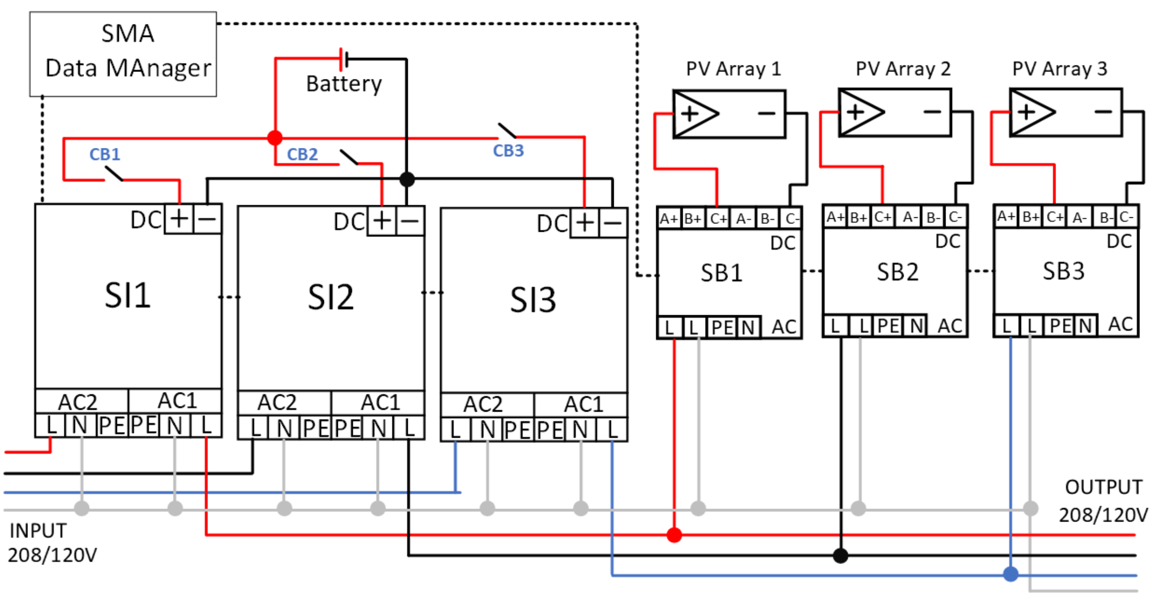

Figure 4-2: Schematic diagram of the PV and battery (SMA) system connections

4.4 Battery powered unit

The left side of figure 4-2 illustrates the wiring connections of the stationary battery and SIs. Each SI has two AC terminals: the Utility Grid/Generator terminal, labeled AC2, and the Load/PV terminal, labeled AC1. These terminals, shown in Figure 4-3, are separated by an isolating relay. Figure 3-5 provides details of the internal connections within the SI and the isolating relay.

As depicted in Figure 4-2, the AC1 and AC2 terminals of the SIs are connected in a Star configuration. This arrangement is essential because this type of SI operates at 120V.

Figure 4-3: power terminals of SI

When any of the SIs detects a deviation in voltage or frequency on any phase of the utility grid/generator (at the AC2 terminal), it notifies the master SI (in this case, SI1). The master SI then opens all isolation relays, disconnecting the AC2 terminals internally from the SIs and AC1. At this point, an isolated nano-grid is formed.

In this nano-grid configuration, if there is a PV power shortage (where load demand exceeds PV generation), the SIs compensate by discharging the stationary battery and supplying AC power. Conversely, if the SBs, with MPPT, generate excess power, the SIs will charge the battery. If the battery becomes fully charged, the master SI initiates **Frequency Shift Power Control (FSPC)** [36].

Under FSPC, the master SI increases the frequency of the islanded nano-grid. As the grid-forming inverter, the SI can adjust the frequency or voltage of the nano-grid. The SBs detect this frequency shift and reduce their PV power generation to maintain the stability of the nano-grid [36].

As shown in Figure 4-4, the SIs are connected to the stationary battery through the splitter box. The switches (CB 1, 2, and 3) shown in figure 4-2 are internal mechanical switches located on the front casing of the SIs, which can be manually turned on or off.

Figure 4-4: Stationary Battery and DC Splitter Box

4.5 Backup Unit

The backup unit includes the EV, the SETEC V2H inverter, and SI4. Its purpose is to inject DC power into the DC bus (via the DC splitter box shown in Figure 4-4) when the stationary battery SoC is low. This approach extends the support time for priority loads. The DC power supplied by the EV can either recharge the stationary battery or support the SIs in compensating for power shortages within the nano-grid.

In this study, the EV is treated as an additional battery storage unit for use in emergencies. The 2015 Nissan Leaf, equipped with a 24kWh battery (comparable to the stationary battery's capacity) effectively doubles the system's backup duration when integrated, if fully charged.

The SETEC V2H inverter plays a crucial role by converting the DC power stored in the EV's battery into 110 VAC. This AC power can then be used to recharge the stationary battery or support the SIs. The necessity of the SETEC inverter arises from the fact that the Nissan Leaf only supplies DC power through its charging terminals when the connected device can communicate with the EV's Battery Management System (BMS). The SETEC inverter is the only available device in this setup capable of communicating with the Leaf's BMS to initiate power transfer.

Once converted to 110VAC, the power must be further converted back to DC for compatibility with the DC bus. While various chargers can be used for this purpose, the SI's battery charging feature is utilized in this system. The main advantages are the SI's controllability of the power limit and its ability to connect with the DM, enabling precise control of power flow from the EV to the DC bus.

4.6 Data and Control Unit

The DM is the central component of this unit, equipped with **ennexOS** to facilitate real-time monitoring and control of the system. It allows observation of instantaneous values, such as voltage and power, and modification of device parameters, such as the intake power of SIs from the utility grid. The DM communicates with SBs and ioLogik via Ethernet and connects to the Master SI through an RS485 port.

Although the DM is not directly connected to the stationary battery's BMS, it can access battery parameters via SI1, which communicates with the battery BMS through CAN. When an SI is connected to a lithium battery, it is essential to select "Lithium battery" as the battery type during the SI configuration process. Without proper communication with the stationary battery BMS, the SI will not operate.

The DM offers the capability to control inputs and outputs, although it does not have built-in input/output terminals. It just includes specific digital inputs designed for controlling or limiting PV generation. To add output terminals to the DM, an ioLogik E1242 module is utilized, with its specifications detailed in Section 4.6 Data and Control Unit.

In this setup, four digital outputs of the ioLogik module are employed, as shown in Figure 4-5. The primary objectives of this circuit diagram are to enable load shedding and regulate the power flow from the EV to SI4. This will be detailed below.

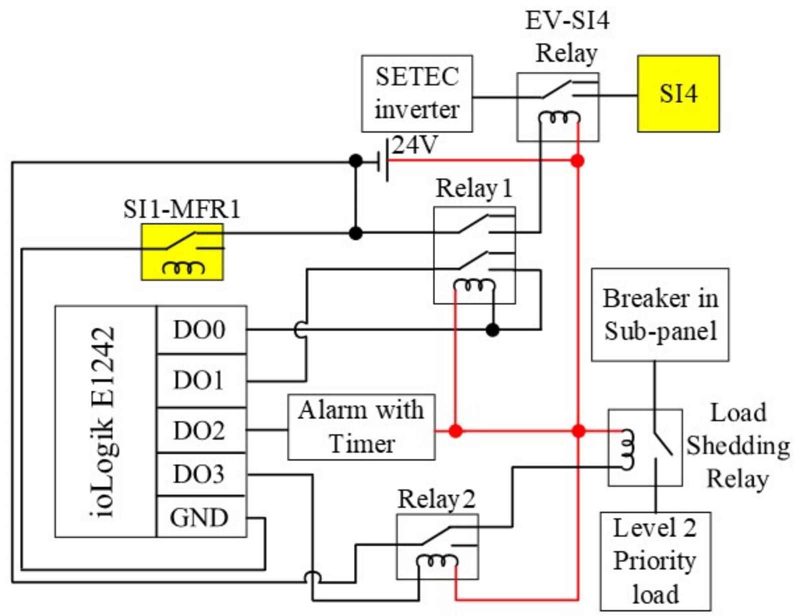

Figure 4-5: ioLogik E1242 digital outputs wiring connection

4.6.1 EV to SI4 Power Flow Control

The components used for EV-SI4 relay control include the EV-SI4 relay, Relay 1, Multi-Function Relay 1 of SI1 (SI1-MFR1), a 24V DC power source, and the ioLogik E1242 module. To ensure that load shedding and EV support to the home are disabled when the utility grid is in normal condition (voltage and frequency within acceptable ranges), SI1-MFR1 is configured to deactivate the ioLogik outputs under normal grid conditions.

The methodology is as follows: Figure 4-6 displays the DM setting page for SI1-MFR1, showing that this relay is programmed to activate when the utility grid is operating normally. This configuration means that during a utility grid fault, SI1-MFR1 is deactivated, causing its common terminal to be connected to the normally closed terminal.

Figures 4-5 and 4-7 illustrate the use of these two terminals on SI1-MFR1. In the event of a power outage, SI1-MFR1 links the negative terminal of the 24V DC power source to the ioLogik. This connection is essential for the functionality of the EV-SI4 relay and load-shedding relay control, as the ioLogik outputs can only be activated during grid faults and are deactivated in normal grid condition.

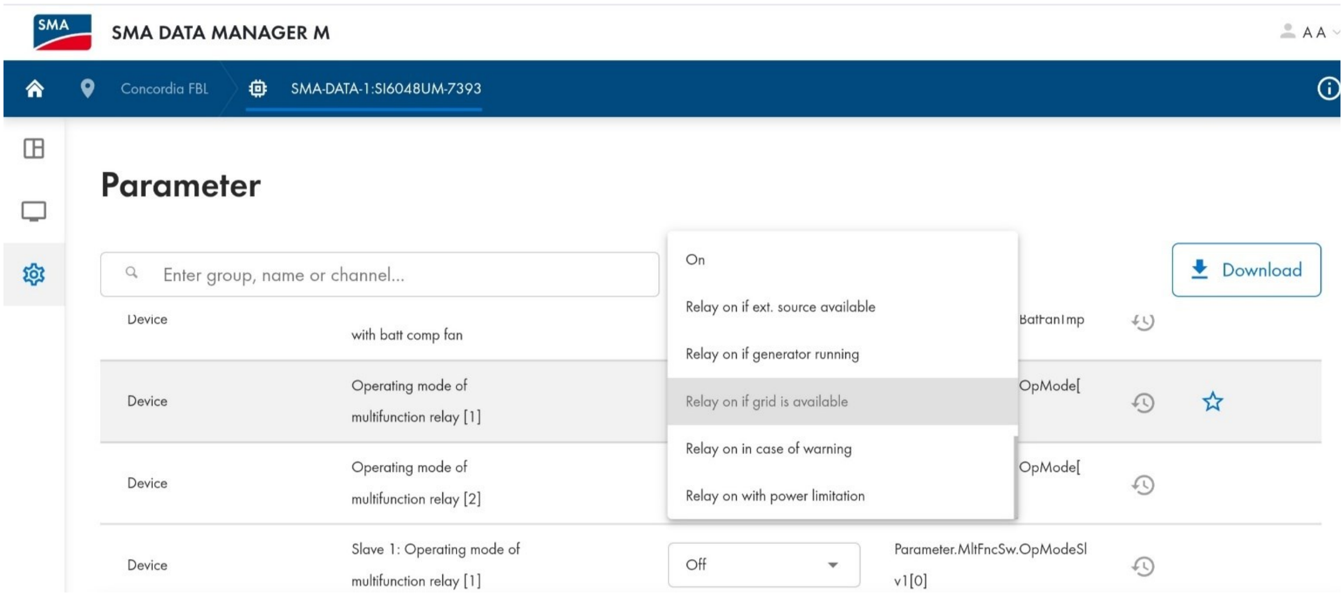

Figure 4-6: DM setting page for SI1-MFR1

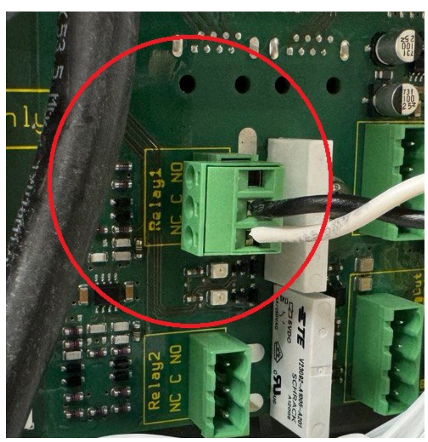

Figure 4-7: SI1-MFR1 terminal

The EV-SI4 relay is set to activate when the stationary battery's SoC drops below 40%. Adding EV power to the system can increase the battery's SoC, potentially causing the EV-SI4 relay to chatter. To prevent this, the EV-SI4 relay is configured to activate when the SoC drops to 40% and deactivate only when it rises to 80%.

Unfortunately, the ioLogik or DM cannot be directly programmed to implement this hysteresis logic. To address this limitation, “Relay 1” and “2 outputs of ioLogik” are used. In the circuit shown in Figure 4-5, **DO0** is set to activate when the battery SoC falls equal or below 40%, and **DO1** is set to activate when the SoC is below 80%.

The behavior of Relay 1 under this configuration for different SoC levels is graphically illustrated in Figure 4-8. In this diagram, **"C"** refers to the common terminal of the relay, "**NC"** to the normally closed terminal, and **"NO"** to the normally open terminal. When an output is activated, it is highlighted in blue for clarity.

1. When SoC = 100%, none of the ioLogik outputs are active.
2. When SoC < 80%, DO1 will be activated. However, this has no immediate effect, as Relay 1 has not yet been triggered.
3. When SoC ≤ 40%, both DO0 and DO1 will be active. The activation of DO0 energizes Relay 1, causing its contacts to switch from NC (normally closed) to NO (normally open). As a result, DO1 is linked to the coil of Relay 1, and terminal “C” is connected to “NO”, activating the EV-SI4 relay.
4. When SoC > 40% (after dropping below 40%), DO0 will deactivate. However, since DO1 is linked to the coil of Relay 1 (as established in step 3) and remains active, it keeps Relay 1 energized. This acts as a latching mechanism, ensuring that Relay 1 remains active. In this condition, terminal “C” stays linked to “NO”, and the EV-SI4 relay remains active. Relay 1 will only deactivate when DO1 is deactivated (i.e., when SoC > 80%).
5. When SoC > 80%, both DO0 and DO1 are deactivated. This deactivates Relay 1, which resets its contacts and deactivates the EV-SI4 relay.

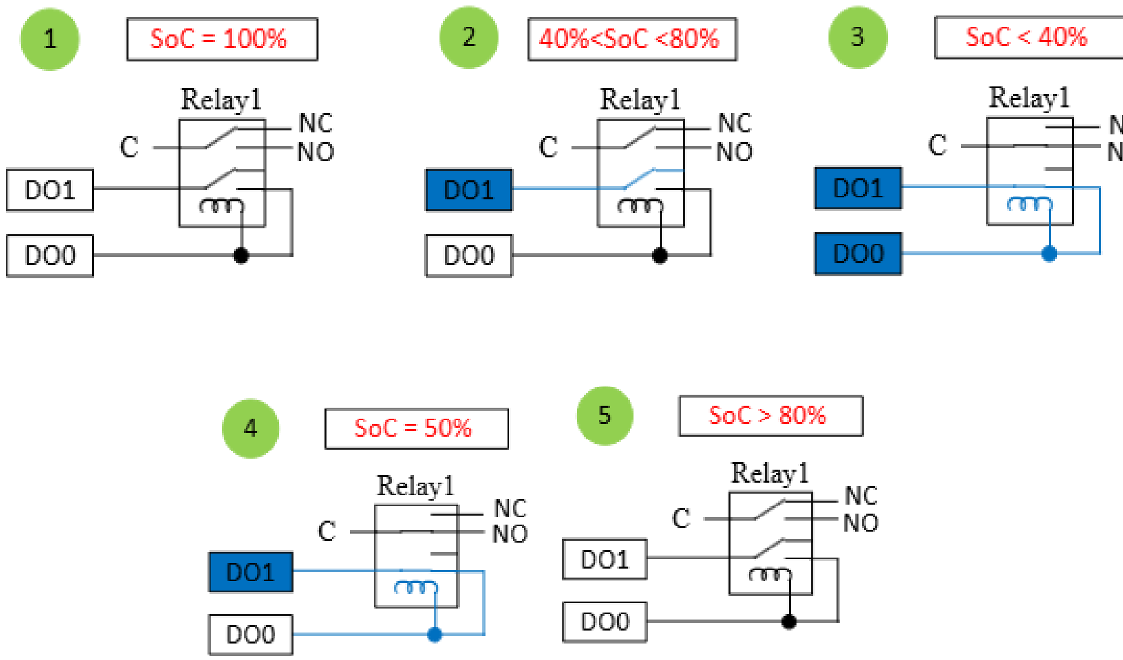

Figure 4-8: changes in relay 1 due to stationary battery SoC variations

It should be noted that in conditions 3 and 4, Relay 1 is activated, linking terminal **"C"** to terminal **"NO"** of Relay 1. This indicates that the EV-SI4 relay is active; thus, SI4 is delivering DC power to the DC bus, charging the stationary battery.

Figure 4-9 illustrates the proposed control circuit for the ioLogik in both normal and faulty utility grid conditions. In the normal utility grid condition, SI1-MFR1 disconnects the ground of the 24V source from the GND terminal of the output of the ioLogik preventing the energization of relay EV-SI4. In the case of a faulty utility grid, the stationary battery's SoC is assumed to be less than 40%, thus DO0 to D01 would be active, that is, connected to the GND terminal of the ioLogiK.

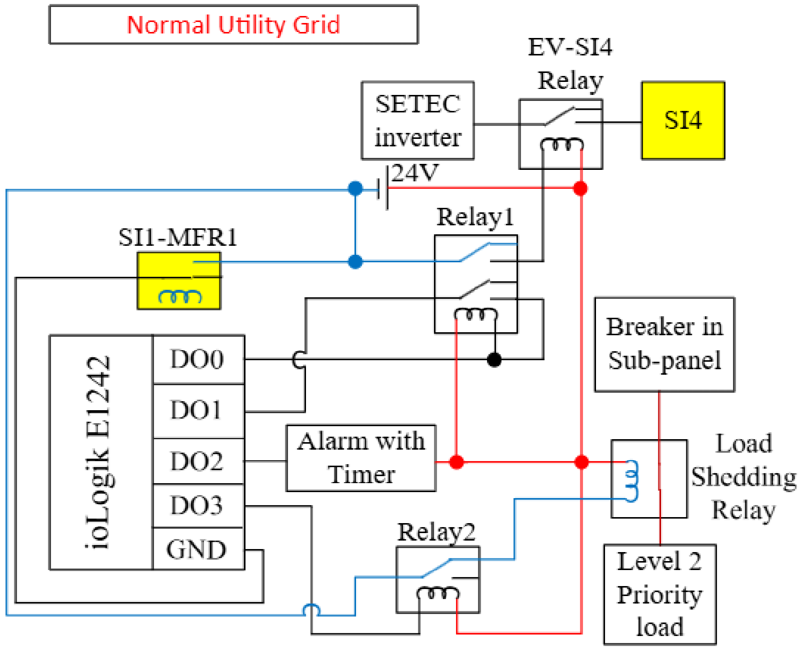

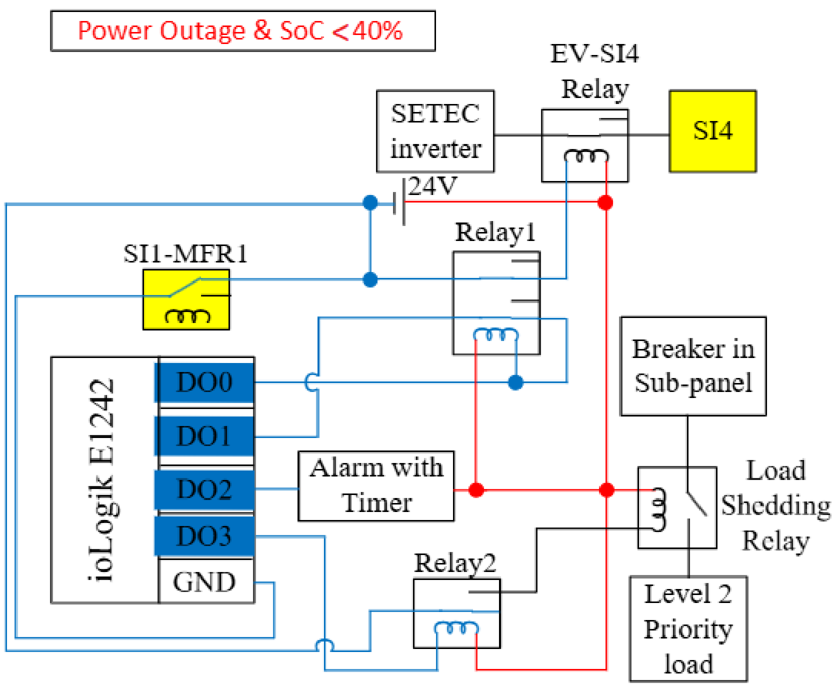

Figure 4-9: proposed control circuit in normal Utility grid versus faulty one (SoC<40%)

To alert the user when the stationary battery SoC is dropping too low and EV connection becomes necessary, an alarm is integrated into the system. DO2 is configured to activate when the SoC falls below a predefined threshold (45%). Upon activation, a timer is triggered, which energizes the alarm for a duration of one minute, providing a clear and timely warning to the user.

4.6.2 Load Shedding

There are two methods available for performing load shedding:

1. Using one of the ioLogik digital outputs, as implemented in this work.
2. Utilizing the Multi-Function Relays (MFRs) of the SIs.

The ioLogik method is preferred in this work because, as described in the previous section, SI1-MFR1 ensures that ioLogik outputs are deactivated during normal grid conditions. This behavior is not exhibited by the MFRs of the SIs. Therefore, using ioLogik allows load shedding to automatically cease when the grid is functioning normally.

Figure 4-10 illustrates the DM setting page used to configure the digital outputs of ioLogik. As shown, DO3 (Digital Output [4]) is configured to activate when the SoC drops to 50% or below. This page is accessible by following Concordia FBL>>Configuration>>Grid Management Services>>Assign Digital Outputs.

Note: Relay 2 functions as a NOT gate, reversing the output of the ioLogik. This configuration is essential because, during normal grid conditions when the loads should remain energized, ioLogik outputs are deactivated by SI1-MFR1. The operation is as follows:

1. Normal Grid Conditions:
    - DO3 is deactivated.
    - Relay 2 is deactivated.
    - Load shedding relay remains active, ensuring the loads are energized.

2. Faulty Grid with SoC > 50%:
    - DO3 is deactivated.
    - Relay 2 is deactivated.
    - Load shedding relay remains active, keeping the loads energized.
3. Faulty Grid with SoC ≤ 50%:
    - DO3 is activated.
    - Relay 2 is activated.
    - Load shedding relay is deactivated, shedding the loads.

Conditions 1 and 3, as described above, are graphically illustrated in Figure 4-9. These conditions demonstrate the behavior of Relay 2 and the load shedding relay under normal grid conditions and during grid faults with SoC < 40%, respectively.

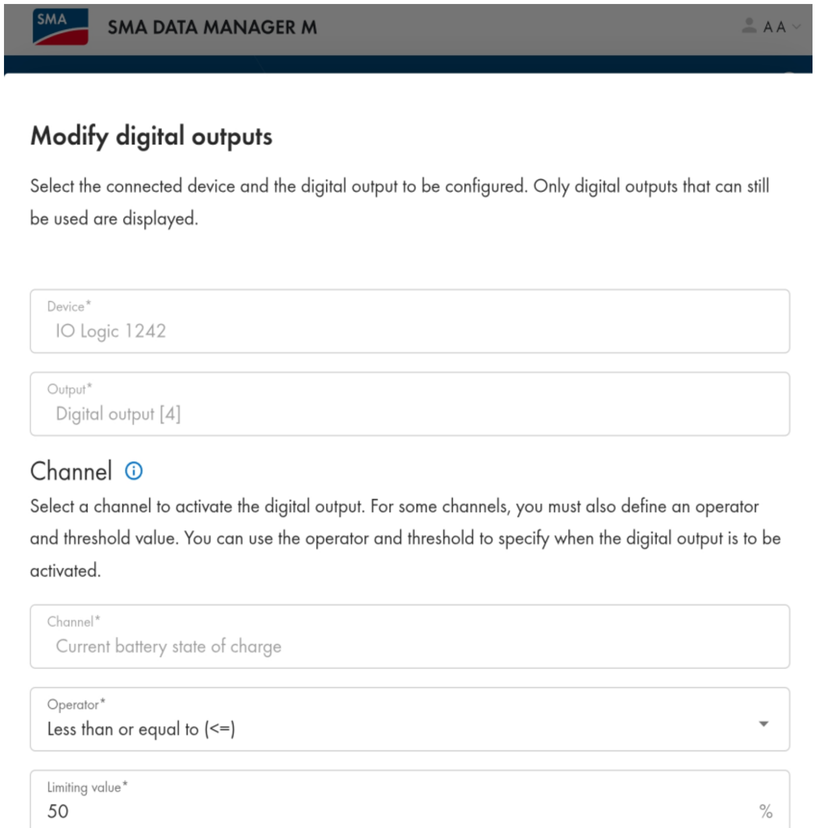

Figure 4-10: DM setting page for DO3 to perform loadshedding

4.6.3 Control of the power drawn from the EV

The ability to control the amount of power flowing from the EV to the system/stationary battery provides users with valuable flexibility for energy management. In this experimental setup, the primary role of SI4 is to offer this controllability.

There are two methods available to control the power delivered by the EV to the system/stationary battery, with both methods can be accessed and adjusted through the display and control buttons on the casing of SI4 or via the DM-ennexOS web interface, which provides remote access to the system's settings and controls.

4.6.3.1 Limiting Intake Power/Current of SI4

The user can set a limit on how much power or current SI draws from the EV, effectively controlling the energy flow into the system.

Through display buttons setting a limit for intake current of SI is accessible by following Settings>>External Settings>>Grid Control>>GdCurNom. Figure 4-11. Shows SI4 display for setting an intake current limit.

Figure 4-11: SI4 display showing intake current limit.

It is also accessible through DM-ennexOS web page by following Concordia FBL>>SMA-DATA-1:SI6048UM-7393>>Configuration>>Parameters>>AC Side>> Maximum Current from Utility Grid. This webpage is shown in Figure 4-12.

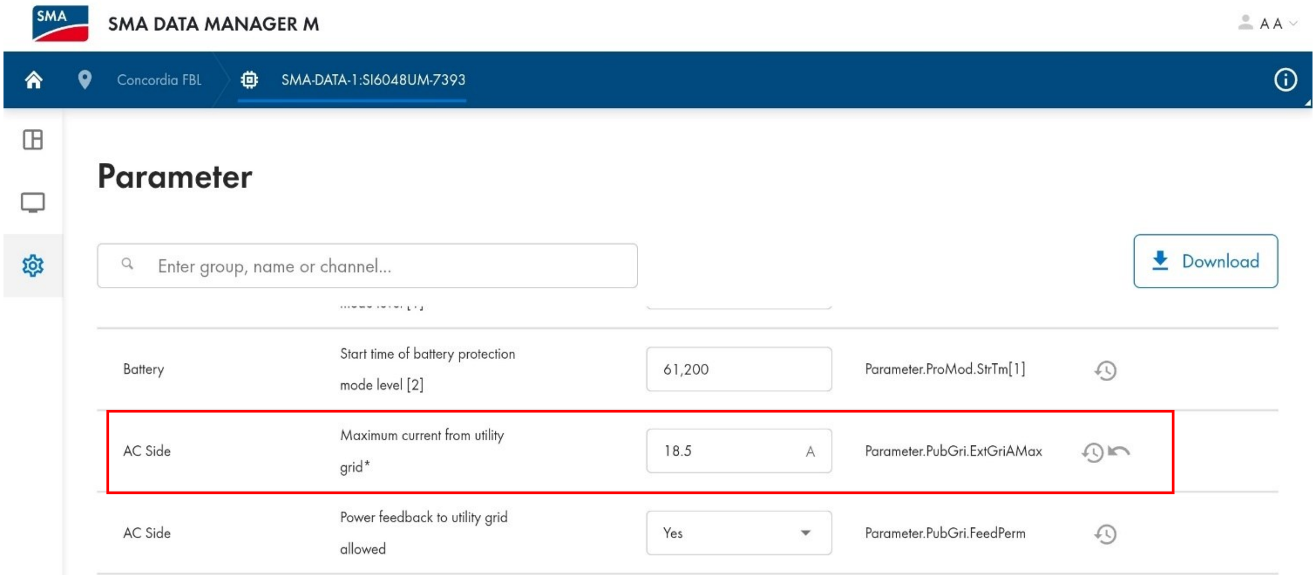

Figure 4-12: DM-ennexOS setting page for limiting SI Intake Current.

4.6.3.2 Limiting the Charging Current of SI4:

The user can control the charging current of SI, ensuring that the power used for battery charging remains within desired limits.

Through display buttons setting a limit for charging current of SI is accessible by following Settings>> Battery Settings>> Battery Charge Mode>>BatChrgMax. Figure 4-13. Shows SI4 display for setting a charging current limit.

Figure 4-13: SI4 display showing charging current limit.

It is also accessible through DM-ennexOS web page by following Concordia FBL>>SMA-DATA-1:SI6048UM-7393>>Configuration>>Parameters>>Battery>> Max. battery Charging Current. This webpage is shown in Figure 4-14.

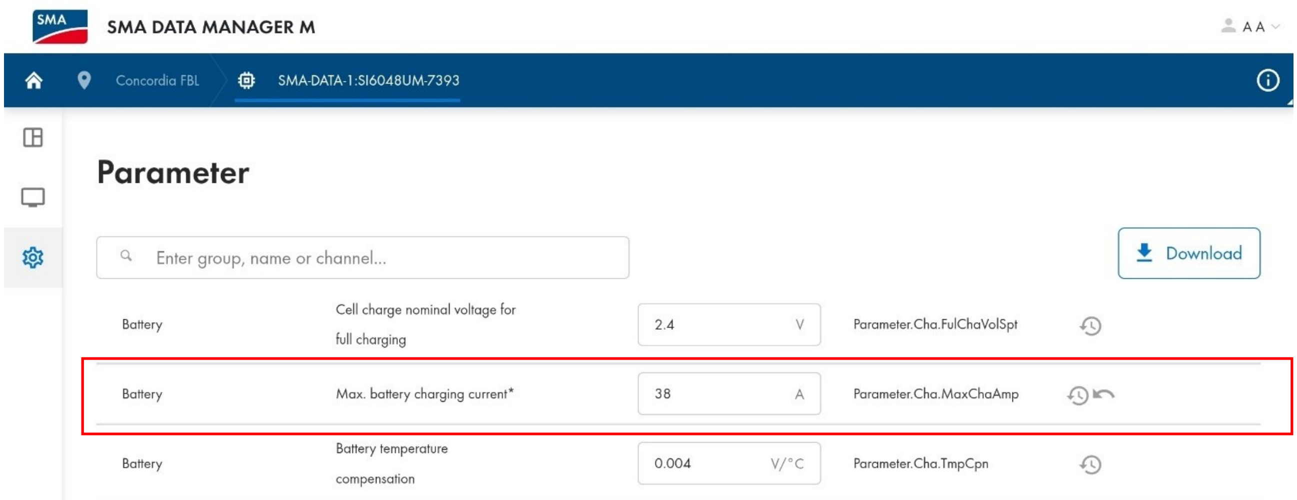

Figure 4-14: DM-ennexOS setting page for limiting SI charging Current.

These options enhance the usability and efficiency of the system, allowing for precise energy management tailored to user needs.

4.7 Challenges and solutions

Several challenges emerged during the preparation of the test setup and the execution of the test. These challenges, along with their respective solutions, are detailed below.

4.7.1 Rooftop PV Arrays

At the time of performing this test, rooftop PV arrays were unavailable. Consequently, a PV emulator and a DC source were utilized as substitutes for PV arrays. Two sources were available for use as PV for the SBs, 1 emulator and 1 DC source. To accommodate the three-phase system using just two SBs, the first SB was configured as a split-phase source (120/240 V_{AC}), while the second SB (SB2) was set up as a single-phase source (120 V_{AC}). This configuration is illustrated in Figure 4-15.

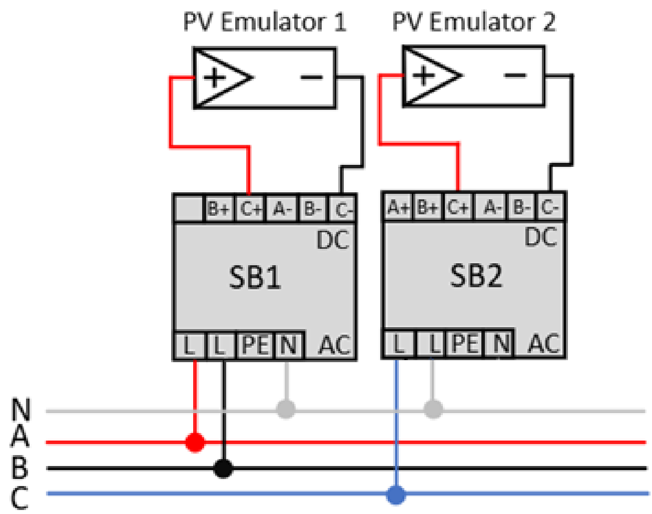

Figure 4-15: PV Emulator Instead of PV Arrays

The PV emulator used to power SB2 be a Chroma 62020H-150S, configured to output a voltage of 150 V and a current of 9 A.

For PV emulator 1, a DC power source (Sorensen DLM 600-6.6), powered through three single-phase isolating transformers, and a series resistor were employed. The circuit diagram of the simulated PV emulator is presented in Figure 4-16.

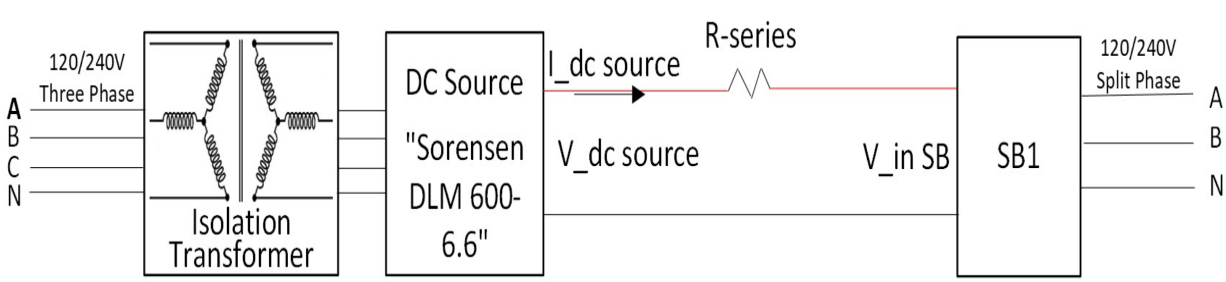

Figure 4-16: Circuit diagram of simulated PV Emulator based on "Sorensen DLM 600-6.6"

In this test setup, the following parameter values were used:

$\mathbf{R}_{\mathbf{series}} = 6.67\ \Omega$, $\mathbf{V}_{\mathbf{dc\text{-}source}} = 350$ V, $\mathbf{I}_{\mathbf{limit\text{-}dc\text{-}source}} = 6.6$ A

4.7.2 SI4 and communication with Battery BMS

4.7.2.1 Battery Configuration in SI

Sunny Island (SI) inverters support various types of batteries, such as Lithium-ion and Lead Acid batteries.

When configuring SI for Lithium-ion batteries, a communication link between the SI and the battery's BMS is essential. This allows the SI to monitor key parameters such as SoC and temperature.

For Lead Acid batteries, external sensors (e.g., current and temperature sensors) may be required based on the system's configuration and desired accuracy. For example, if a PV panel is directly connected to the battery, adding a current sensor is necessary since the SI cannot measure the PV-generated current without that sensor.

In this test setup, SI1, SI2, and SI3 form a single cluster 3-phase, with SI1 functioning as the master. However, SI4 operates independently while being connected to the same battery. Since SI4 is not a slave of SI1, it requires a direct connection to the battery BMS for communication.

4.7.2.2 Configuration Challenge

In this test setup, both SI1 and SI4 are connected to the same Lithium-ion battery. Ideally, both inverters should be configured for Lithium-ion batteries. However, SMA advises against connecting two master SIs to the same battery BMS. Moreover, when a Sunny Island (SI) is configured to operate with a Lithium-ion battery, it requires a functional communication link with the battery BMS to operate. If the communication link is missing or disconnected, the SI will either fail to start or, if it is already operating, it will cease functioning.

4.7.2.3 Solution

To address this, the following approach was adopted:

SI1 was configured for a Lithium-ion battery. This is critical as it is the MASTER SI of the three-phase cluster, and DM reads battery data from SI1.

SI4 was configured for a Lead Acid battery. While this setup causes minor inaccuracies, such as an incorrect SoC reading on SI4, these are not critical in this specific test setup.

4.7.2.3.1 Justification for SI4 Configuration

Overcharging Concerns: Although SI4 displays an incorrect SoC, the higher SoC limit (as described in Section 4.6) is user-defined and controlled by SI1, DM, and the ioLogik. These devices have accurate SoC readings, ensuring proper control of the EV-SI4 relay.

Battery Protection: The Lithium-ion battery is equipped with a BMS that provides overcharge and over-discharge protection, mitigating potential risks associated with incorrect SoC readings from SI4.

By configuring SI4 for a Lead Acid battery, the system's functionality and safety are maintained, while adhering to the limitations of SMA's recommendations.

4.8 Alternative Experimental Setup

In the experimental setup described above, the EV power is integrated into the system at the DC bus/stationary battery connection through the charger of SI4. An alternative configuration for connecting the EV power is illustrated in Figure 4-17. In this configuration, V2L inverter is planned to be directly connected to AC2 side (utility grid/generator) of SI1 in case of utility grid failure.

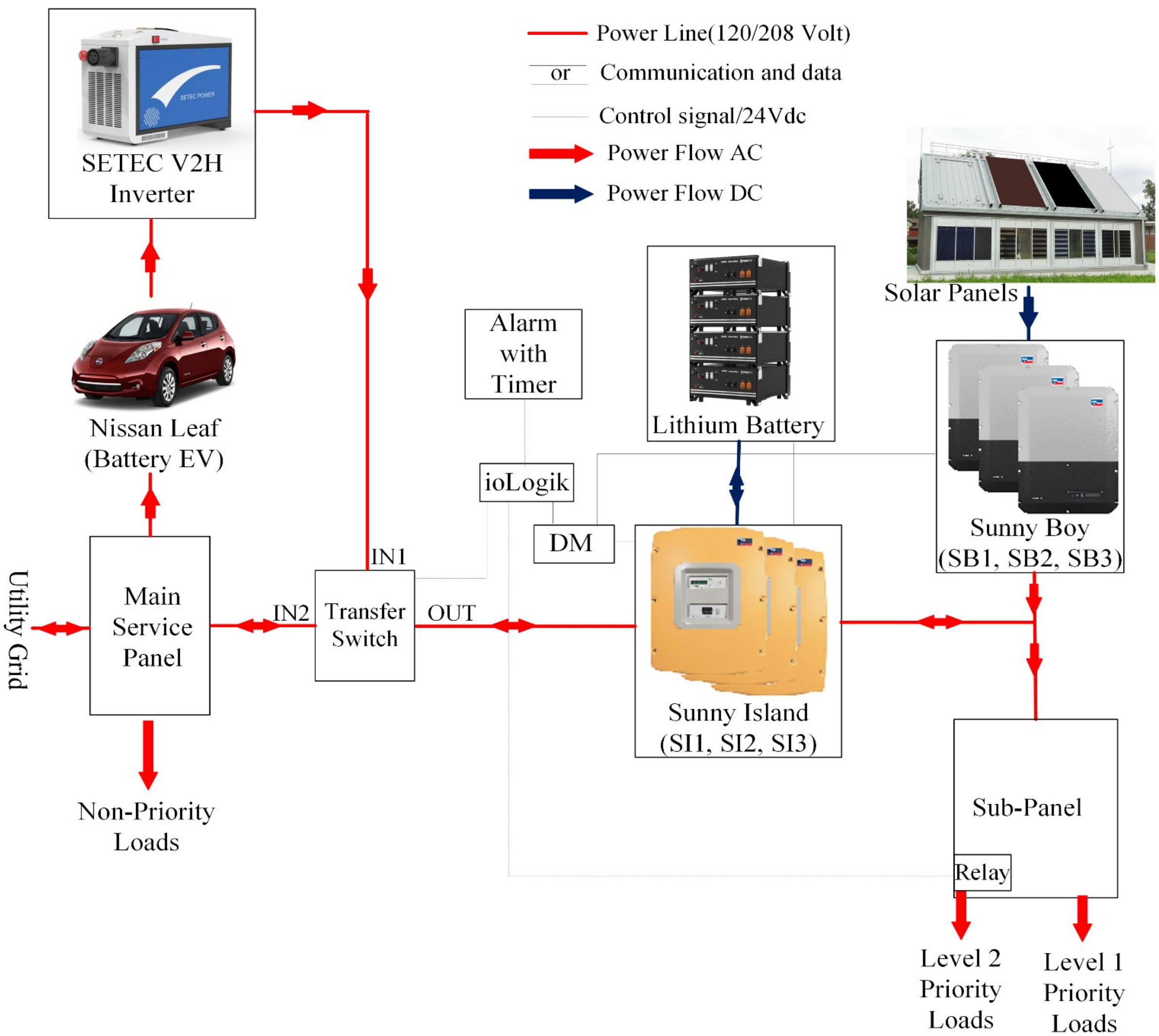

Figure 4-17: Alternative experimental setup

In the current setup, SI1, SI2, and SI3 form a three-phase single cluster, with SI1 acting as the master SI. The SIs continuously monitor the voltage and frequency at the grid/generator-side terminal. If any deviation occurs outside the specified limits (upper/lower), the master SI disconnects all isolation relays. This poses a challenge when connecting a single-phase V2L inverter to the three-phase SMA cluster because:

1. When a single-phase V2L inverter is connected to SI1, two out of three SIs (SI2 and SI3) are not connected to the source and will measure zero voltage at their grid-side terminals (AC2).
2. This triggers the master SI to open all isolation relays, disconnecting the cluster from the V2L inverter.

As a result, it appears impossible to directly connect a single-phase V2L inverter to a three-phase SMA cluster.

Proposed Solution: Sequential Connection Procedure

To enable the connection of a single-phase V2L inverter to a three-phase SMA cluster, the following steps can be employed:

1. **Turn Off SI2 and SI3**:
   - Temporarily shut down the slave SIs (SI2 and SI3) via the manual switch on the casing (this switch is highlighted in figure 4-18), leaving only the master SI (SI1) active.
2. **Connect V2L Inverter to Master SI (SI1) through transfer switch**:
   - Connect the single-phase V2L inverter to the master SI by changing the position of transfer switch.
   - Since only SI1 is operational, it will measure the grid-side voltage and frequency from the V2L inverter.
   - If the V2L inverter's voltage and frequency fall within acceptable limits, SI1 will close its isolating relay, connecting the V2L inverter to the load side and the SI1 charger.

3. **Turn On SI2 and SI3**:

- Once the V2L inverter is successfully connected, SI2 and SI3 can be powered on by closing the manual disconnect switches located on their casings.
- The slave SIs (SI2 and SI3) will then communicate with the master SI (SI1) and synchronize to its frequency and phase angle.
- SI2 and SI3 will subsequently provide the appropriate phase angles required to complete the three-phase operation.
- After being powered on, SI2 and SI3 detect that there is no external source on their grid/generator side and switch to grid-forming mode. In this mode, they either discharge the battery to supply the load side or, if there is surplus PV generation, charge the battery.
- A potential question may arise: why don't the SIs disconnect the V2L inverter in this configuration, as was mentioned earlier? It appears that after SI2 and SI3 are manually turned on, they interpret SI1 as forming a grid. As a result, they do not report any faults on their grid/generator sides to the master SI. This behavior may stem from the possibility that such a scenario was not accounted for in the SIs' programming by the manufacturer.

By following this procedure, it becomes possible to integrate a single-phase V2L inverter into a three-phase SMA cluster. This approach ensures compatibility and allows the V2L inverter to contribute to the system effectively while maintaining the operation of the three-phase cluster. However, the process remains manual and requires careful execution to avoid operational issues.

Figure 4-18: Disconnect Switch on the casing of SI

4.8.1 Benefits of Alternative over Proposed Experimental Setup:

4.8.1.1 Eliminating SI4

The primary advantage of the alternative configuration over the proposed experimental setup is the elimination of SI4. In this alternative scheme, the V2L inverter is connected directly to the AC bus instead of the DC bus of the stationary battery, through SI4, as in the original setup. In the alternative setup, the transfer switch changes the AC input source of SIs from utility grid (in normal conditions) to V2L inverter (in grid failure conditions). In grid failure, the transfer switch connects the single phase V2L inverter to SI1. Here, SI2 and SI3 will not be directly supplied by V2L inverter.

4.8.1.2 Loss reduction

Connecting the V2L inverter to the AC side of SI1 eliminates the need for voltage rectification and reduction, which simplifies the system and reduces energy losses. Thus, improves efficiency while maintaining the functionality of integrating the EV into the system.

4.8.2 Drawback of Alternative Experimental Setup

4.8.2.1 Lack of Automation

The primary drawback of this alternative scheme is its lack of automation; the entire process is completely manual (detailed in 4.8). This limitation requires user intervention to manage the connection and operation of both the V2L inverter and the SMA inverters (SIs), making the system less convenient and potentially unreliable in critical situations.

4.8.2.2 Lack of Controllability Over the Power Drawn from the EV through SETEC V2L Inverter

The available V2L inverter lacks programmability, meaning the user cannot directly control its output or intake power. However, in the experimental setup discussed in Section 4.1, the power drawn from the EV can be effectively controlled/limited by the user through SI4.

This though can be performed through SI1. It is possible to limit the intake power of SI1 as is discussed in 4.6.3. This will lead to limit/control over EV intake power.

This limitation may cause inconvenience because, after a power outage, the intake power from utility grid/ generator side must be adjusted or eliminated. When the utility grid returns to normal, the stationary battery requires recharging, and load shedding will cease. This results in a change in demand between power outage conditions and normal grid conditions, necessitating different limitations on intake power to accommodate the new requirements.

4.8.3 Interesting feature of 3-phase SI cluster in Alternative Setup.

In this scheme, it is possible to limit the power drawn from the V2L inverter by controlling the input current of SI1. When a SI is connected to an external power source, such as a V2L inverter, it may share the intake power between the load side and battery charging. For example, if the intake power of SI1 is limited to 2 kW and its load side consumes 500 W, the remaining 1.5 kW may be used to charge the battery. When a cluster of SIs is formed, they share a common battery bank via a shared DC bus, as illustrated in Figure 4-19.

Now, as shown in Figure 4-19, assume SI1 is limited to drawing 2 kW from the V2L inverter, and the SI cluster is connected to a balanced 1.5 kW three-phase load. In this scenario, by neglecting losses, the 2-kW output from the V2L inverter is evenly divided between the three load/phases and the battery bank. In other words, a single-phase V2L inverter is effectively supporting a three-phase load.

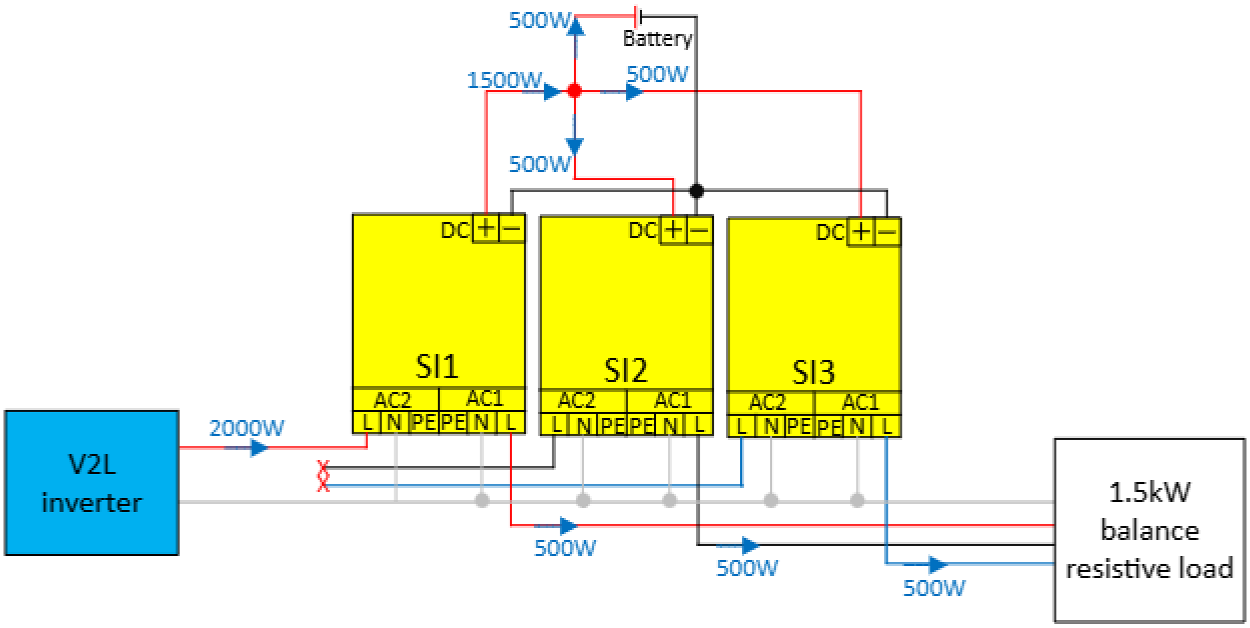

Figure 4-19: SI cluster with common battery

This feature has been tested and has proven to work effectively.

4.8.4 Data and Control Unit (Alternative Experimental Setup)

The same ioLogik interface detailed in Section 4.6, with some minor modifications, can be used in this configuration. The modified diagram is shown in Figure 4-20. The primary difference is that in the new interface, the ioLogik signals control the transfer switch, changing transfer switch position from the utility grid (during normal grid conditions) to the V2L inverter (during faulty utility grid conditions). The transfer switch will receive a signal to switch to the V2L inverter only when the utility grid is faulty, and the battery SoC drops to 40%. The switch will remain in this position until the battery SoC reaches 80%, at which point the system will adjust accordingly.

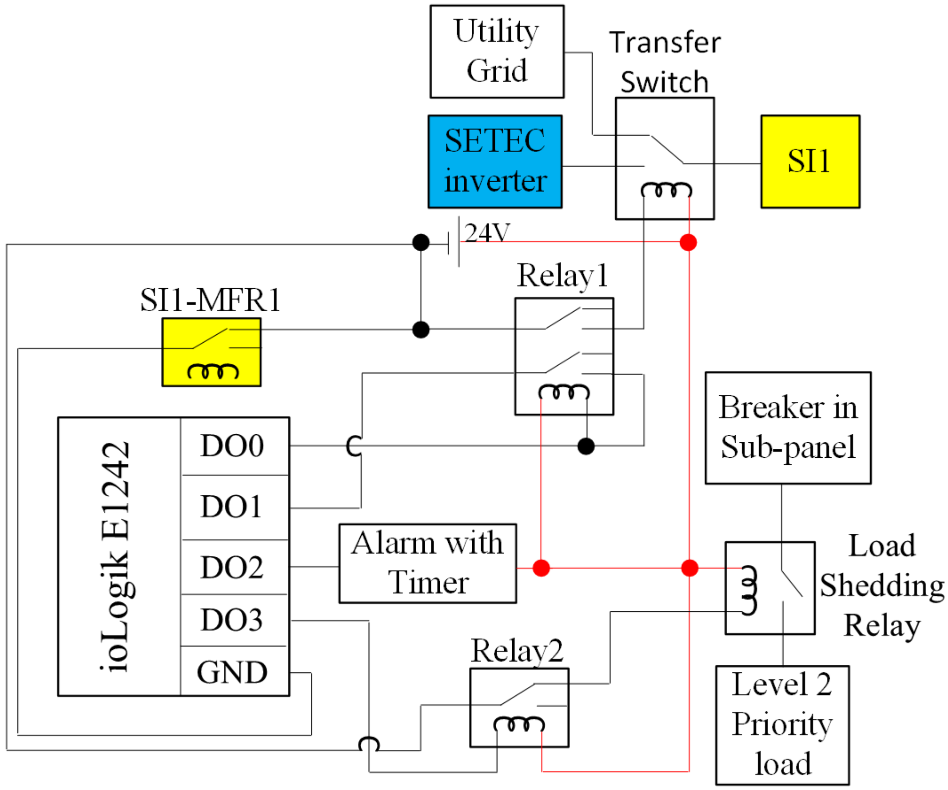

Figure 4-20: Modified ioLogik Interface for alternative Experimental Setup

4.9 V2G with Available Experimental Setup

The experimental setup detailed in Section 4.1 can be upgraded to support V2G functionality. Following this concept will be described.

To allow electricity to be fed from the DC side of an SI into the utility grid, the battery voltage of a charged battery must be increased beyond the "nominal charging voltage." This can be achieved by using external DC chargers or the Sunny Island Charger to boost the battery voltage above its standard charging threshold [36].

The above mentioned V2G topology works based on the above-mentioned fact. This means that if SI4 is used as the external charger, the battery voltage will be boosted through charging via SI4. Once the voltage reaches the required level, SI1-3 begin delivering power to the utility grid. In this configuration, the V2L inverter effectively operates as a V2G inverter, indirectly contributing power to the grid.

To achieve this, the same electrical connection presented in Figure 4-1 can be utilized with eliminating the Alarm system, ioLogik and load shedding relay. The proposed electrical connection to enable V2G capability in the SMA system is illustrated in Figure 4-21.

In addition to these modifications in figure 4-21, the control unit and its programming must be updated to accommodate this change. These adjustments are necessary to manage the increased battery voltage effectively and facilitate the seamless transfer of electricity from the DC side to the utility grid. This ensures the system operates reliably and efficiently in a V2G configuration.

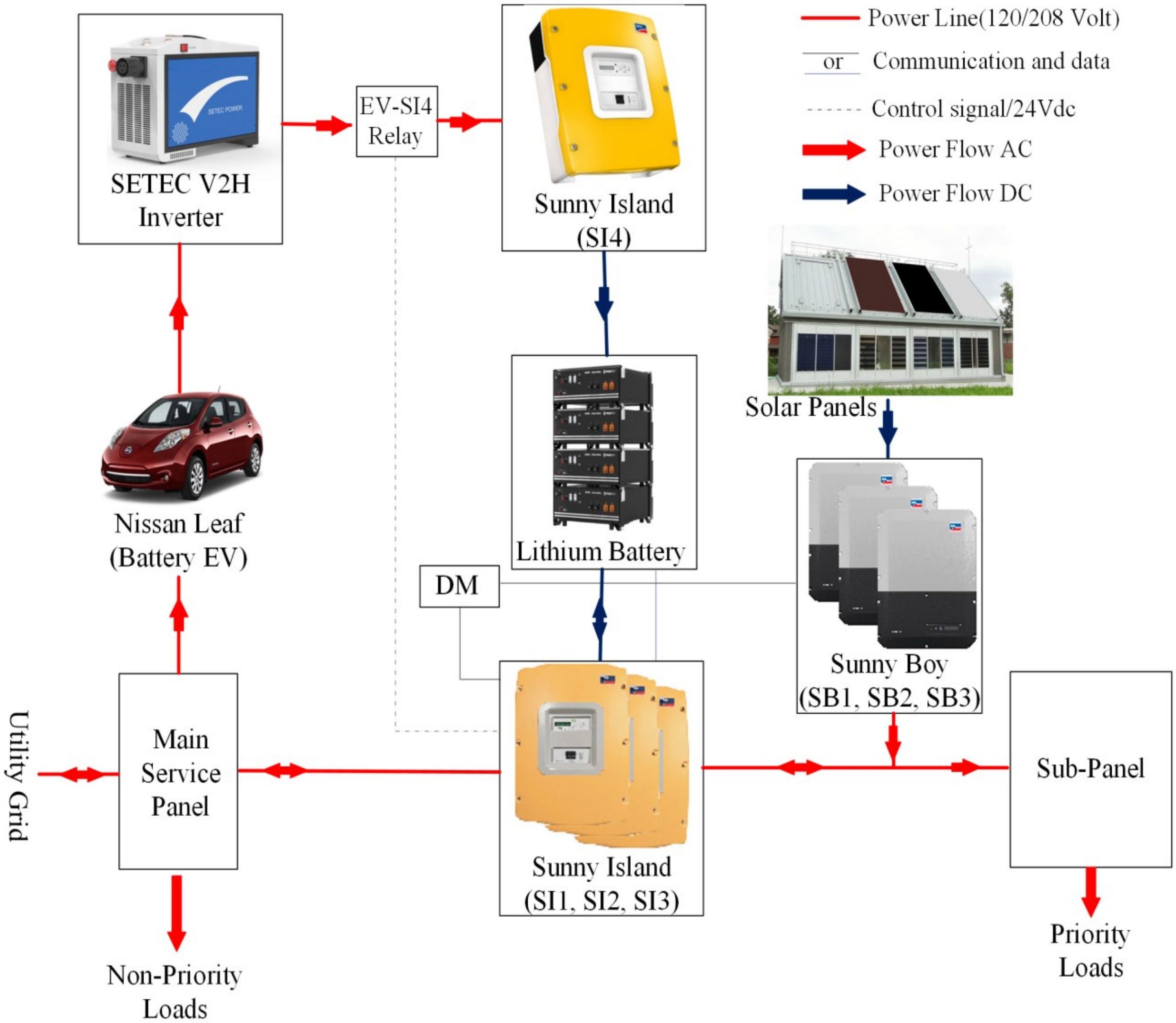

Figure 4-21: Experimental Setup with V2G Capability

4.9.1 Critical condition (Control Unit)

A critical situation arises when there is a failure in the utility grid. If a failure occurs, the three main SIs will open their isolating relays, meaning they can no longer transfer the DC surplus power delivered by SI4 to the utility grid. This scenario could result in different issues depending on the battery type:

- **Lead-acid batteries** could experience overcharging since the excess power cannot be transferred to the grid. In this setup, SI4 will protect Lead Acid battery from overcharging. Thus, it should not make any issue with lead acid batteries.
- **Li-ion batteries**, on the other hand, might disconnect from the system in response to the surplus power. This way all system would experience unwanted shutdown.

  Li-ion batteries are equipped with a Battery Management System (BMS) that protects them from both overcharge and over-discharge situations, preventing damage to the battery.

To prevent such a situation, the best solution would be to disconnect EV-SI4 relay in case of grid failure. Figure 4-22 shows the proposed control interface.

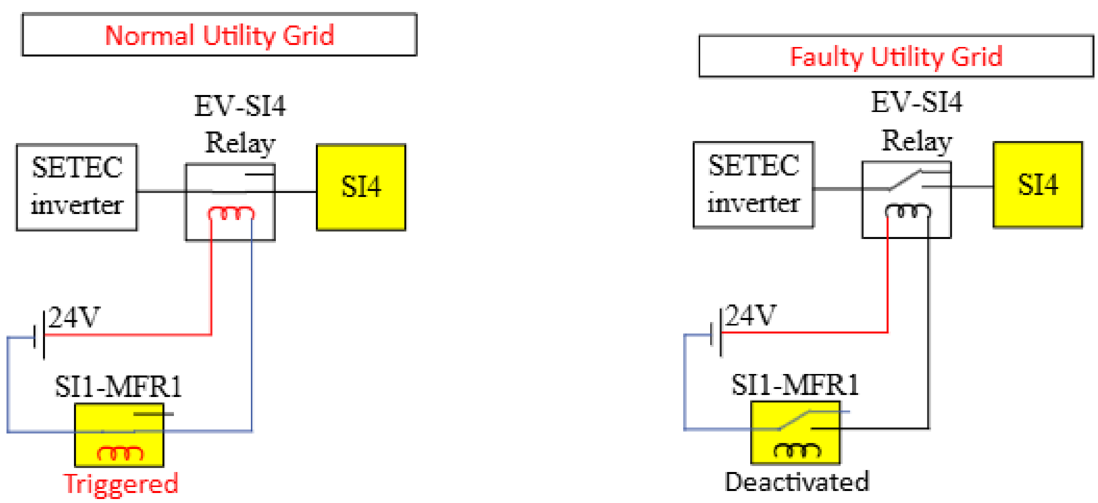

Figure 4-22: Figure 4-17. Control interface to control EV-SI4 relay

As discussed in Section 4.6.1, SI1-MFR1 can be programmed to activate under normal utility grid conditions. If the Common and Normally Open (NO) terminals of SI1-MFR1 are configured as shown in Figure 4-22, the following occurs:

- **Normal Utility Grid (Left Side of Figure 4-22):**
    - SI1-MFR1 activates, linking the GND of the 24V DC source to the coil of the EV-SI4 relay, triggering the relay.
    - This action connects the V2L inverter to SI4, starting the charging process.
- **Faulty Utility Grid (Right Side of Figure 4-22):**
    - SI1-MFR1 deactivates, disconnecting the GND from the EV-SI4 relay coil.
    - As a result, the EV-SI4 relay is deactivated, stopping the power flow from the V2L inverter to SI4.

This configuration ensures that the EV-SI4 relay and the power flow from the V2L inverter are automatically managed based on the utility grid's status.

Note: Since this setup is designed to operate when the utility grid is functioning normally and the SIs are connected to the utility grid, Load Shedding becomes unnecessary in this context. Furthermore, as discussed earlier, SI1-MFR1 is sufficient for grid detection and controlling the EV-SI4 relay, eliminating the need for the ioLogik interface.

This simplification has been implemented in the proposed electrical connection shown in Figure 4-21 and 4-22.

4.9.2 Flexibility

The ability to control or limit the power that SI4 draws from the EV, allows for precise regulation of the power injected from the EV into the utility grid. This means that the power flow from the EV to the utility grid can be actively monitored and controlled, providing flexibility and efficiency in V2G operations.

Controlling the power flow from the EV to SI4 is discussed in detail in 4.6.3.

An SI is primarily a grid-forming inverter but also has the capability to operate as a grid-following inverter. Figure 3-5 illustrates the internal connections of SI. For better clarity, the internal connections of the SI, along with the utility grid, SB, and load, are depicted in Figure 4-23.

As shown in Figure 4-23, under normal utility grid conditions, the bi-directional inverter of the SI operates as a grid-following inverter, synchronizing with the utility grid's characteristics, such as voltage, frequency, and phase angle, similar to a SB but bi-directional.

In contrast, during faulty utility grid conditions, the isolation relay disconnects the utility grid entirely from the nano-grid. In this scenario, the SI transitions to a grid-forming inverter, providing voltage and frequency references for the nano-grid.

This dual functionality means the SI can operate as both a grid-forming and a grid-following inverter.

When the SI is functioning as a grid-following inverter, the power injected into the utility grid represents the net power of the nano-grid. In other words:

Net Power = EV/SI power (delivered via SI) + PV power – Load Power

This is shown in figure 4-24.

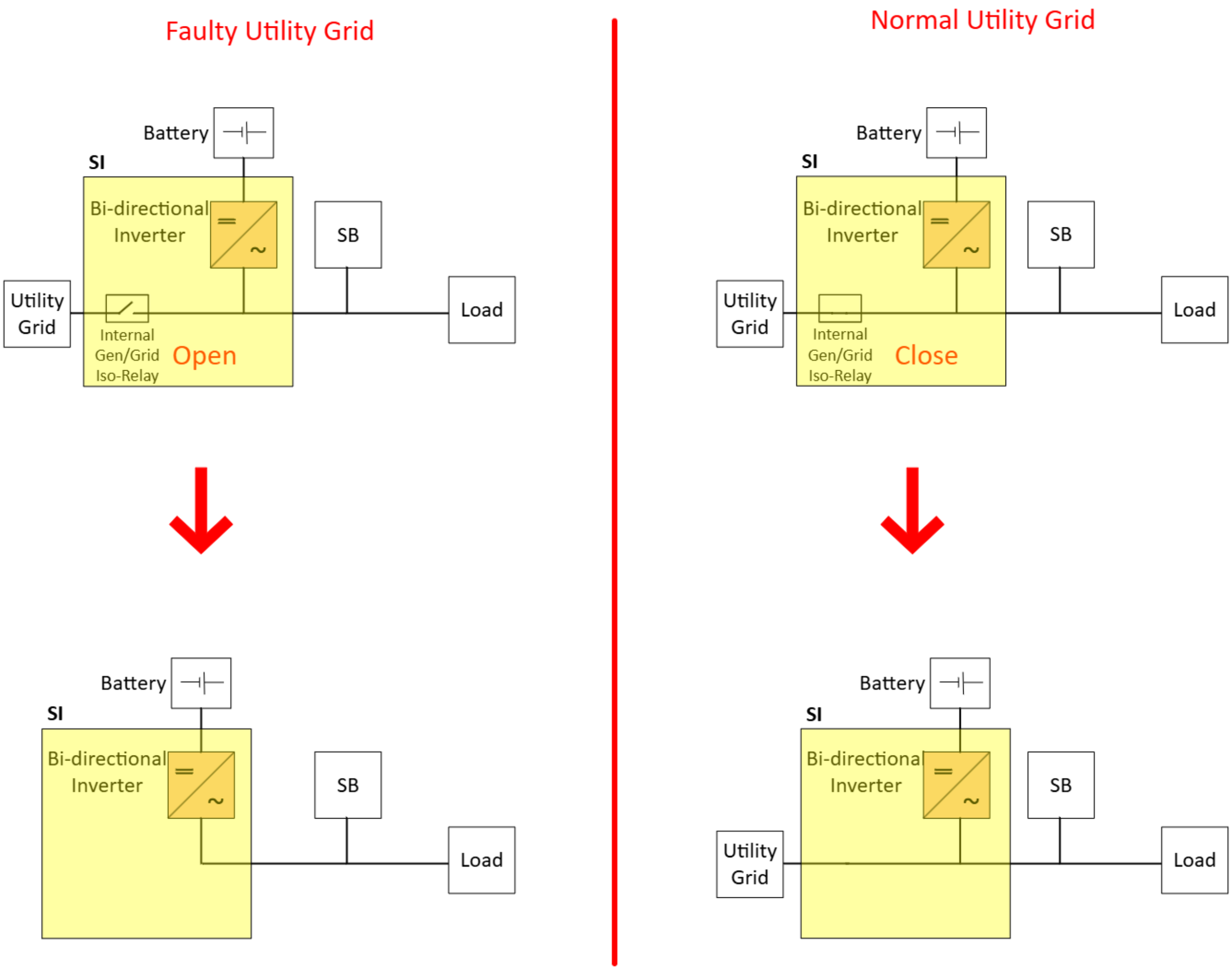

Figure 4-23: Islanded and Grid connected SI.

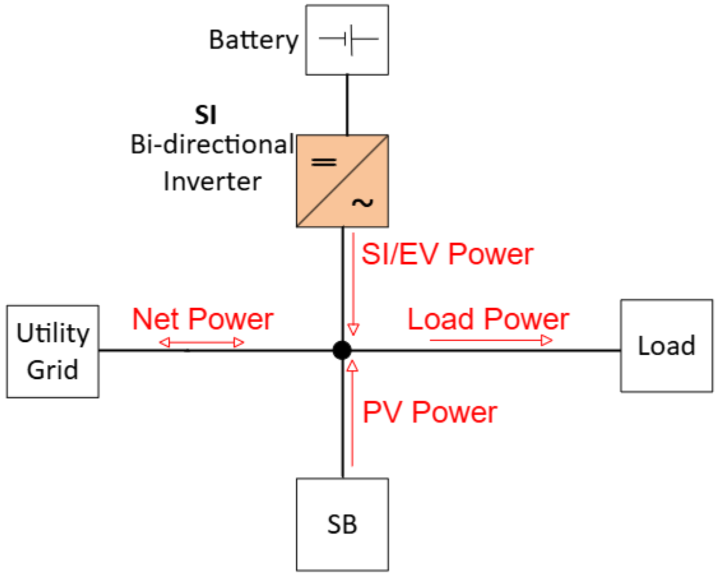

Figure 4-24: Net Power in V2G Scheme

Note: The SI includes a feature that allows it to limit the intake power from the utility grid while operating in the grid following mode. This functionality is achieved through Power Monitoring and Adjustment:

- The SI continuously monitors the power drawn from the utility grid.
- If the power demand from the load side of the SI, exceeds the preset limit, the SI compensates by injecting the excess power from the battery.
- If the power demand from the load is less than the limit, the SI may charge the battery while respecting the preset limit of power being drawn from the utility.

Example:

If the power limit is set to 2 kW and the load side demand is 3 kW, 2 kW comes from the utility grid and the SI provides the additional 1 kW by discharging the battery.

Once the condition where load demand exceeds the limit has passed, the SI resumes charging the battery. For instance, if the load side demand decreases to 1 kW after previously being 3 kW, the SI will charge with the remaining 1 kW of the 2kW provided by the utility.

This feature allows the SI to act as a power stabilizer in weak grids by smoothing out power fluctuations and ensuring the load demand does not overburden the grid. This functionality is particularly beneficial for enhancing grid reliability and resilience in areas with unstable power supply.

Chapter 5 - Energy management Strategy

5.1 Introduction

The proposed procedure for having the EV battery supporting the AC nano-grid under critical utility outage conditions is divided into 7 stages. It should be noted that according to the duration of the power outage and load consumption, the system may witness only a few of the 7 stages. Herein, the stages are described in more details.

5.2 Normal Utility Grid

In this stage (Stage 1), the utility grid is operating under normal conditions, meaning it is regulating both voltage and frequency. All loads, including the priority loads, are supplied by the utility grid as well as by the power generated from the PV panels during the daytime.

The internal isolation relays of SI1, SI2, and SI3 remain closed in this mode, connecting the SIs directly to the utility grid. In this configuration:

- The SIs operate as grid-following inverters/chargers, synchronized with the utility grid's voltage, frequency, and phase angle. This is detailed in 4.9.2.
- The utility grid takes precedence as the primary energy source for the connected loads, while any additional power generated by the PV panels is either consumed by the loads or used to charge the battery.
- If the battery is not fully charged and there is surplus energy available (either from the grid or PV generation), the SIs automatically switch to charging mode, directing the excess power to the battery storage.

This operational stage ensures that the energy demands of all loads are met efficiently while maximizing the utilization of PV-generated power and maintaining the battery in a charged state. It also provides a seamless transition to support the system during unexpected utility grid faults, as the battery remains ready to supply backup power if needed.

5.3 Faulty Utility Grid

This stage (Stage 2) begins immediately following a power outage, causing the utility grid to become unavailable. As a result, the internal isolation relays of SI1, SI2, and SI3 automatically open, disconnecting the utility grid from the system. This would occur immediately.

In this condition, the SIs transition to **grid-forming mode**, taking over the role of regulating voltage and frequency within the nano-grid. The SIs manage the balance between the power generated by the SBs and the power consumed by the three-phase priority loads.

The grid-forming operation leads to the following:

- If the power generated by the SBs exceeds the load demand, the SIs direct the surplus energy to charge the battery, causing the SoC to increase.
- Conversely, if the load demand surpasses the power generated by the SBs, the SIs compensate by discharging the battery, leading to a decrease in the battery SoC.
- If the battery is fully charged and there is a power surplus in the isolated grid, the SIs increase the reference frequency. The Sunny Boys (SBs) detect this frequency shift and respond by reducing their PV power generation. This adjustment ensures that the net power in the isolated grid becomes zero, preventing overcharging or energy imbalance.

This operational stage highlights the importance of the battery and SIs in maintaining uninterrupted power to priority loads, ensuring resilience and stability during utility grid outages.

5.4 Load Shedding

If the SoC of the battery drops below 50%, stage 3 starts. Load shedding is implemented to save battery energy and support higher priority loads (Level 1 priority loads in figure 4-1) for extended periods. The SoC of the battery is continuously informed to the DM by the SI1. As the

SoC drops below 50%, the Digital Output (DO3) of the ioLogik is activated, which triggers Relay 2, and consequently deenergizes the coil of the “load shedding relay” as indicated in Figure 4-9. The load shedding relay is a certified relay in North America. it is a normal open relay that disconnects the Level 2 priority load when deenergized. As is discussed in 4.6.2, during normal utility grid condition, all outputs of the ioLogik are deactivated. Besides, the ground terminal of the 24 V source, that energize the control coils of the relays is not connected to the output ground terminal of the ioLogik because relay SI1-MFR1 inside SI4 is used in the way to be open during normal Utility Grid. It is closed following a grid fault.

5.5 Alarm Activation

If the SoC of the battery continues to decrease and falls below 45%, the system enters Stage 4. This stage signals that the EV needs to be prepared for connection to the islanded grid to support the system and extend the time which Level 1 priority loads can remain powered. To prompt this action:

An alarm connected to DO2 of the ioLogik is triggered when the SoC drops to 45%. This alarm serves as a warning to the operator or homeowner, alerting them to connect the EV to the V2H inverter.

A 1-minute timer is integrated into the alarm functionality. This timer ensures the alarm remains active long enough to effectively capture the operator's attention and prompt immediate action, without staying active for an excessive duration that might disturb residents.

5.6 EV Connection for Support

Stage 5: Since the SIs shut down at a SoC of 30% (Lead Acid Battery), the power transfer from the EV to SI4 and subsequently to the stationary battery begins when the SoC drops to 40% via activating and closing the EV-SI4 relay. The V2H inverter, energized in the previous stage, remains operational, while SI4 is continuously powered.

5.6.1 Three Possible Conditions after EV connection

5.6.1.1 EV Delivered Power + PV Generation Exceeds Load Demand

In this condition, the combined power from the EV and PV generation surpasses the load demand. The surplus power is used to charge the stationary battery, leading to an increase in its SoC. To prevent chattering (frequent on/off switching) and protect the battery from overcharging, the protection/control interface described in Section 4.6 and shown in Figure 4-5 is implemented. This interface is programmed to:

- **Activate** the EV-SI4 relay when the SoC drops to **40%**.
- **Deactivate** the relay and halt charging when the SoC rises to **80%**.

5.6.1.2 EV Delivered Power + PV Generation Matches Load Demand

In this scenario, the combined power generation from the EV and PV system is approximately equal to the load demand.

The system achieves a balance, and there is no need to draw from or charge the stationary battery. As a result, the battery's SoC remains stable around 40%.

5.6.1.3 EV Delivered Power + PV Generation is Less Than Load Demand

When the combined power from the EV and PV system falls short of the load demand, the deficit is drawn from the stationary battery. This causes the battery's SoC to drop below 40%.

If this condition persists and the SoC falls below 30% (Lead Acid Battery), SIs will shut down, triggering the following sequence:

- The SIs stop operating, causing the SBs to disconnect from the grid.
- With the SIs no longer providing the reference voltage, frequency, and phase synchronization required for the SBs, the **islanded grid** loses its power sources.
- As a result, priority loads are de-energized, leaving them without power.

5.7 EV Shutting Down

Stage 6: If the SoC of the EV battery falls below 30%, the V2L inverter, that communicates with the EV battery, shuts down to protect the EV battery. If this happens while the SoC of the stationary battery is bigger than 30%, one returns to stage 2 (section 5.3). If the SoC of the stationary battery falls below 30% prior to that of the EV battery, SI1 the master SI, shuts the system down.

5.8 Returning to normal Utility Grid conditions

Stage 7: If the grid returns to its normal condition, there would be 2 possibilities as below:

5.8.1 SIs are <u>active</u> at the time of the utility grid returning to normal conditions

Assuming the SoC of the stationary battery is above 30%, this stage begins when the utility grid returns to normal operation. At this point:

- Any ongoing power flow between the EV and the stationary battery stops.
- Ends load shedding, allowing all loads to operate normally.
- The SIs resynchronize with the utility grid, and the internal isolation relays of SI1, SI2, and SI3 close. The SIs transition back to grid-following mode, recharging the battery as needed.
- Following this process, the system returns to Stage 1, where all loads, including priority loads, are fed by the utility grid and PV generation.

5.8.2 SIs are <u>OFF</u> at the time of the utility grid returning to normal conditions

If, prior to the utility grid returning to normal, the SoC of the stationary battery dropped below 30%, the SIs would have shut down automatically, leaving the entire islanded grid de-energized.

When the utility grid is restored:

1. Manual Restart of SIs:

   The SIs do not turn on automatically. Thus, the user must manually restart them by pressing and holding the "Enter" button on SI1 (master) casing.

2. Reconnection to Utility Grid:

   Once manually restarted, the SIs' isolation relays close, allowing the utility grid to feed the loads and provide a reference for voltage, frequency, and phase angle.

3. Synchronization of SBs:

   With the reference from the utility grid, the SBs begin synchronizing. During daytime, the SBs deliver PV power to the nano-grid.

4. Battery Charging:

   If sufficient power is available in the nano-grid (from PV or the utility grid), the SIs will resume charging the battery to restore its SoC.

This sequence ensures the smooth transition of the system back to normal operation after a critical shutdown caused by low battery SoC.

Chapter 6 - Test Results

6.1 Introduction

The proposed configuration, control strategy and system implementation for allowing an EV with a single-phase V2L inverter to support a three-phase hybrid Photovoltaic plus battery nano-grid was tested experimentally at Concordia's Future Buildings Laboratory (FBL). The goal was to verify its performance and accuracy following a power outage. The test results are provided and discussed in this chapter. The test was performed in two different scenarios:

1. **Long-term test:** the power outage lasted for an extended period. As a result, the EV was connected to the system to charge the stationary battery up to the preset limit. Once the battery reached this limit, the EV was disconnected.
2. **Short-term test:** The power outage ended during the charging process, causing the EV to be disconnected and the load shedding terminated.

Table 6-1 shows the values of system parameters used in this test.

Table 6-1: System Parameters

Parameter	Value
Level 1 priority loads	3480W ~3.5 kW
Level 2 priority Loads	1270W ~1.3 kW
PV generation	3035W ~3 kW
EV-SI4 charging power	2010W ~2 kW
Stationary battery capacity	21 kWh
EV battery capacity	24 kWh

As a measurement tool, the display of the Sunny Island inverter (SI4), employed for charging the stationary battery from the EV shown in figure 6-1, and the DM ennexOS webpage, shown in Figure 6-2 were used.

a. Charging Current

b. Battery Voltage

Figure 6-1: SI4 Display

6.2 Modifications in performing the test

At the moment of writing the paper, the rooftop PV panels were not yet available for testing. As a result, a scheme with only two PV emulators, one of 2 kW and another of 1 kW was used for testing. The first and larger one was connected to MPPT input C of SB1 (SB1 was connected to phases A-B) while the second was connected to MPPT input C of SB2 (SB2 was connected to phase C and neutral). Since the SBs operate inherently independently, there were no problems, and the SIs of each phase managed the unbalanced power injections. Figure 4-15 illustrates the implemented wiring connections. This is detailed in section 4.7.1.

To decrease the overall time of this test, the SoC levels mentioned in chapter 5 were modified as follows.

- Load shedding was activated at 95% of SOC, instead of 50%.
- The enabling of power flow from the EV to the stationary battery, via V2L inverter and SI4, occurs at 94% of SOC instead of 40% while
- Its disconnection takes place for an SOC of 98% instead of 80%.
- In this test, the alarm is also activated at SOC = 95% to have time to connect EV to SETEC inverter.

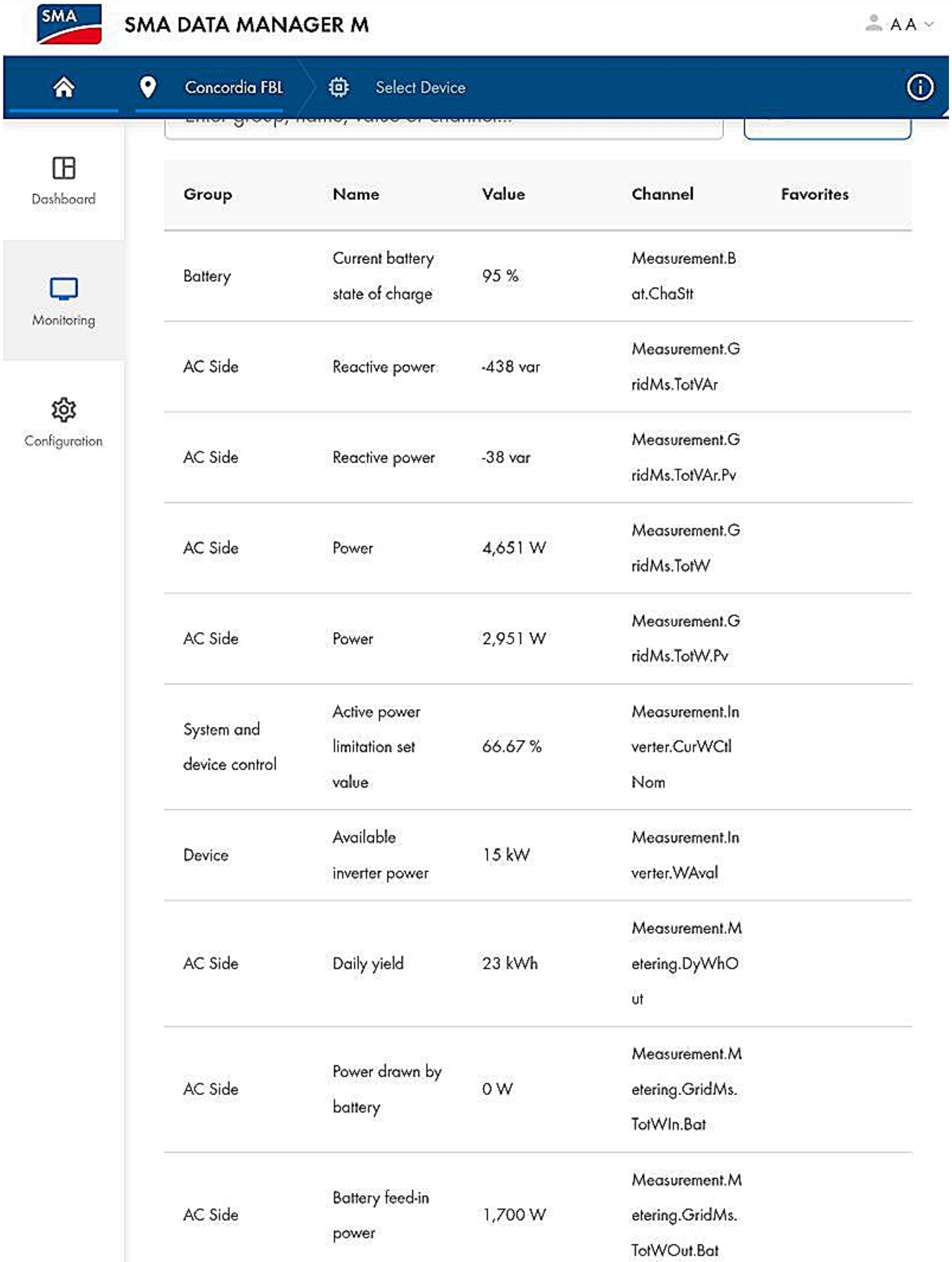

Group	Name	Value	Channel	Favorites
Battery	Current battery state of charge	95 %	Measurement.Bat.ChaStt	
AC Side	Reactive power	-438 var	Measurement.GridMs.TotVAr	
AC Side	Reactive power	-38 var	Measurement.GridMs.TotVAr.Pv	
AC Side	Power	4,651 W	Measurement.GridMs.TotW	
AC Side	Power	2,951 W	Measurement.GridMs.TotW.Pv	
System and device control	Active power limitation set value	66.67 %	Measurement.Inverter.CurWCtlNom	
Device	Available inverter power	15 kW	Measurement.Inverter.WAval	
AC Side	Daily yield	23 kWh	Measurement.Metering.DyWhOut	
AC Side	Power drawn by battery	0 W	Measurement.Metering.GridMs.TotWIn.Bat	
AC Side	Battery feed-in power	1,700 W	Measurement.Metering.GridMs.TotWOut.Bat	

Figure 6-2: DM ennexOS webpage

6.3 Test Results

As mentioned in Section 6.1, the test was conducted under two conditions. The primary objective of the long-run test was to evaluate the overall performance of the proposed method, particularly the ioLogik. The second test aimed to validate the functionality of the multifunction relay of the master SI in managing the charging by EV process and load shedding. The results are presented herein.

6.3.1 Test results for long-run power outage conditions

Figure 6-3 shows the following quantities of the system under consideration: SoC of the stationary battery, load demand, PV generated power, SIs injected power, and EV-SI4 delivered power. These are measured every minute. The small fluctuations observed in Fig.6-3 b are due to the MPPT feature of the SBs.

Following the grid fault at t = 0 minutes, the load demand of 4.8 kW exceeds the PV power generation of 3 kW, causing the battery inverters to supplement the PV inverters. As a result, the SoC of the stationary battery begins to decrease.

At t = 34 minutes, the battery SoC reaches 95%, triggering the ioLogik to open the level 2 priority load relay, disconnecting 1.3 kW of load. Although this reduces the power shortage to 500 W, the load demand still exceeds the PV supply. Consequently, the battery SoC continues to decline, at a slower rate. Simultaneously, an alarm is activated for one minute to alert the operator to connect the SETEC V2L inverter to the EV.

At t = 61 minutes, the SoC decreases to 94%, prompting the ioLogik and the proposed circuitry to close the EV-SI4 relay. This action initiates a 2kW power flow from the EV to the stationary battery. With the load demand and PV generation remaining nearly constant, there is now a net positive power flow of approximately 1.5 kW into the stationary battery, causing its SoC to increase.

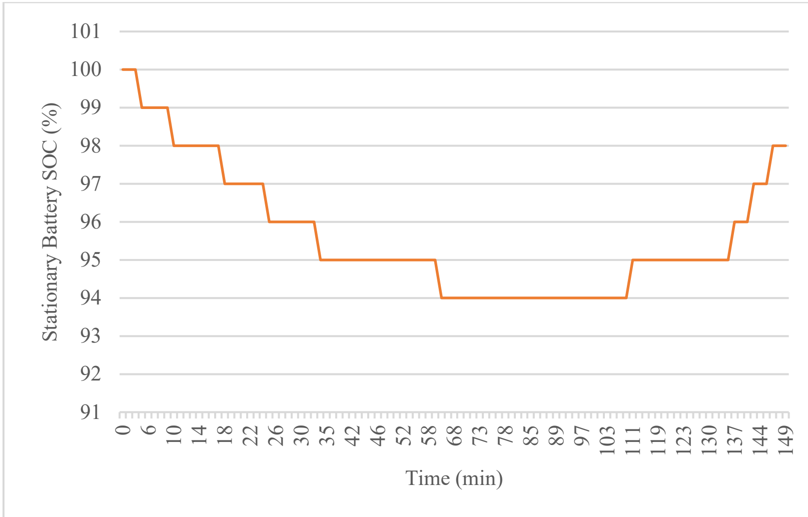

a. Stationary Battery Soc Versus Time

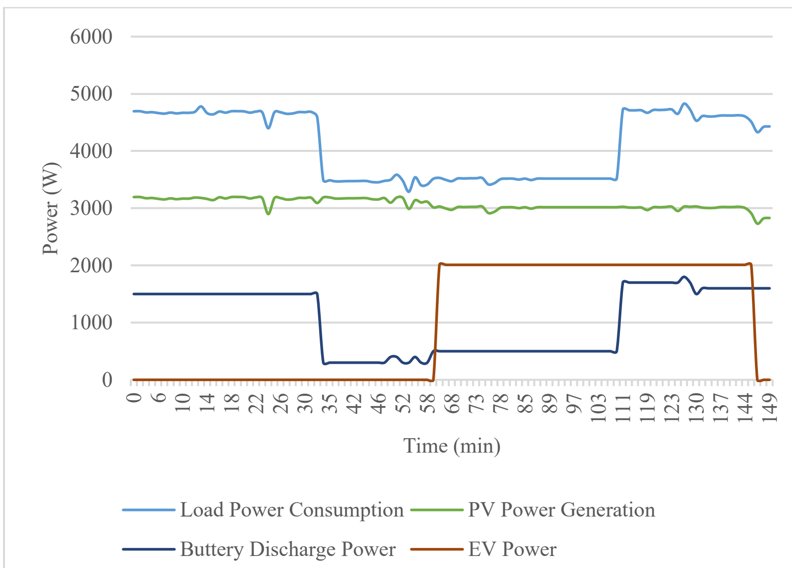

b. Power Measurement Versus Time

Figure 6-3:Measured Parameters-Test 1

At t = 111 minutes, the SoC reaches 95%, resulting in the end of load shedding. The reconnection of the previously shed loads increases both the total load demand and the power injected by the SIs into the AC bus. Despite this, the 2kW drawn from the EV allows the SoC of the stationary battery to continue increasing.

Finally, at t = 146 minutes, the SoC reaches 98%, which triggers the ioLogik to deactivate the EV-SI4 relay, halting the power flow from the EV to the stationary battery.

These results validate the feasibility and functionality of the proposed algorithm and the implemented scheme as well as the proposed configuration of ioLogik.

6.3.2 Test results for short-term power outage conditions

The test parameters, including PV generation and load demand, are listed in Table 6-1 and remain the same as in the first test. In this test, the grid was planned to return to normal conditions shortly after the EV was connected (SOC ≤ 94%). This timing was chosen to ensure that both load shedding and EV charging were activated at the time of grid restoration which is the primary objective of this test to validate the performance of the multifunction relay of the master SI. Test results are illustrated in figure 6-4.

Following the grid fault at t = 0 minutes, the load demand of 4.8 kW exceeds the PV power generation of 3 kW, causing the battery inverters to supplement the PV inverters. As a result, the SoC of the stationary battery begins to decrease.

At t = 33 minutes, the battery SoC reaches 95%, triggering the ioLogik to open the level 2 priority load relay, disconnecting 1.3 kW of load. Although this reduces the power shortage to 500 W, the load demand still exceeds the PV supply. Consequently, the battery SoC continues to decline, at a slower rate. Simultaneously, an alarm is activated for one minute to alert the operator to connect the SETEC V2L inverter to the EV.

At t = 60 minutes, the SoC decreases to 94%, prompting the ioLogik and the proposed circuitry to close the EV-SI4 relay. This action initiates a 2kW power flow from the EV to the stationary battery. With the load demand and PV generation remaining nearly constant, there is now a net positive power flow of approximately 1.5 kW into the stationary battery, causing its SoC to increase.

At t = 65 minutes, the utility grid returns to normal condition by energizing the SIs feeder from the main panel. At this point, charging by EV and load shedding continue. Thus, all parameters remain the same as previous step.

After 5 minutes at t=65 minutes, the master SI links all isolation relays along with multifunction relay 1 of SI1. The latter disconnects the GND of ioLogik, effectively terminating both EV charging and load shedding. By doing so, the drawn power from EV drops to 0, Load demand increases to 4.8kW, PV generation remains 3kW, 6.6 kW is drawn from utility grid, and battery is charged by 4.8kW.

Note: After the grid returns to normal, it takes 5 minutes and 15 seconds for the SI to change the state of the isolation and multifunction relay. However, since the time resolution in this test is set to one minute, its impact is represented in the graphs as 5 minutes. On the other hand, after power outage, these changes in multifunction relay and isolation relays take place immediately.

Note: In these tests, load consumption, PV generation, and power intake from the utility grid and EV are considered positive values. Power drawn from the stationary battery is also considered positive, while charging power is considered negative.

The results confirm the functionality of the multifunction relay of SI1 in terminating the entire process upon the return of the utility grid to normal conditions.

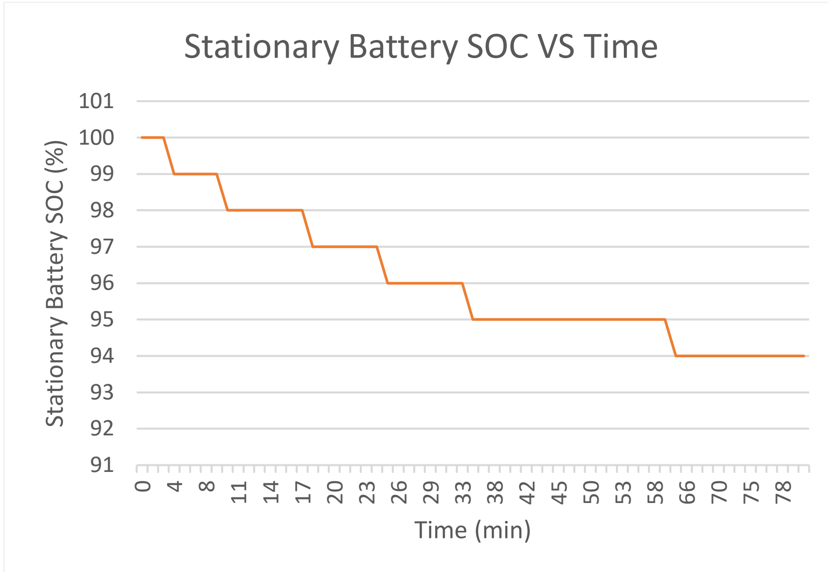

a. Stationary Battery Soc Versus Time

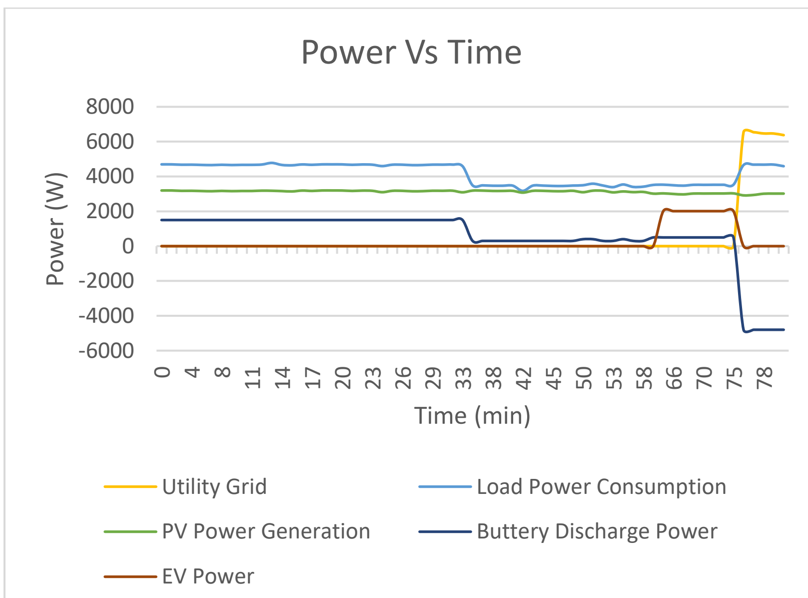

b. Power Measurement Versus Time

Figure 6-4:Measured Parameters-Test 2

6.4 Resilience comparison

This section discusses the resilience of the SMA system in supplying priority loads, both with and without the integration of an EV battery, under long-term and short-term test conditions. It is important to note that the resilience index (introduced in 1.11) is influenced by several variables, including the duration of the power outage, the energy management strategy, and the implementation of load shedding. Variations in any of these factors can significantly impact the resilience index. Therefore, in this test, the variables are kept constant. It should be noted that determining the optimal values for energy management is beyond the scope of this study. Instead, the objective is to demonstrate that the proposed method contributes to an overall improvement in system resilience. In this analysis, a state of charge (SOC) threshold of 94% is defined as the shutdown point of the system. This modification in shutdown SOC is intended to reduce the test run time.

6.4.1 Resilience in long-term power outage conditions

Without EV

In the absence of EV integration, the system shuts down upon reaching an SOC of 94%. According to the graphs presented in Figure 6-3, after power outage, both priority loads (totaling 4.8 kW) are energized for the initial 34 minutes, followed by only the Level 1 priority load (3.5 kW) for an additional 27 minutes. The total test duration remains 151 minutes, with a reference load of 4.8 kW. Using Equation 1-2, the calculated resilience index in this scenario is **R=0.36**.

With EV

According to the graphs presented in Figure 6-3, during the first 34 minutes following the power outage, both Level 1 and Level 2 priority loads—totaling 4.8 kW (3.5 kW + 1.3 kW)—remain energized. Subsequently, load shedding is activated, and only the Level 1 priority loads (3.5 kW) are supplied for the next 77 minutes. After this period, load shedding is deactivated, and both priority loads are once again energized for the remaining 40 minutes until the system returns to normal operating conditions. The total test duration is 151 minutes, with the total priority load of 4.8 kW. Based on Equation 1-2, the calculated resilience index for this scenario is **R=0.86**.

As evident from the results, the resilience index increases significantly from **0.36** to **0.86** with the integration of the EV battery into the system.

6.4.2 Resilience in long-term power outage conditions

Without EV

In the absence of EV integration, the system shuts down when the state of charge (SOC) reaches 94%. According to the graphs presented in Figure 6-3, following power outage, both priority loads (totaling 4.8 kW) are fully energized for 33 minutes, followed by only the Level 1 priority load (3.5 kW) for an additional 27 minutes (load shedding). The total reference load is 4.8 kW, and the total evaluation period is 65 minutes. Using Equation 1-2, the calculated resilience index in this scenario is **R=0.81**.

With EV

According to the graphs shown in Figure 6-3, during the first 33 minutes following the power outage, both Level 1 and Level 2 priority loads—totaling 4.8 kW—are energized. Subsequently, load shedding is activated, and only the Level 1 priority load (3.5 kW) remains energized for an additional 32 minutes, until the utility grid returns to normal operation. The total reference load is 4.8 kW, and the total evaluation period is 65 minutes. Based on Equation (1-2), the calculated resilience index for this scenario is **R=0.87**.

conclusion:

The experimental results confirm the feasibility and effectiveness of the proposed algorithm and the implemented scheme. In both test scenarios, the resilience index of the system improved with the integration of the EV battery, although the degree of improvement varied. It is important to note that the extent of this improvement depends on the duration of the power outage. This is because the primary role of the EV is to support priority loads once the stationary battery reaches a low state of charge (SOC). If the SOC threshold is not reached during the outage, the resilience indices of the systems with and without EV integration remain the same.

Chapter 7 - Conclusion and Future Work

7.1 Introduction

This chapter presents the conclusions drawn from this research and highlights the effectiveness of the proposed energy management strategy in enhancing system resilience through EV integration. Additionally, this chapter outlines potential directions for future work, including optimization of the energy management strategy, integration of additional distributed energy resources, and the development of adaptive control methods to further enhance system resilience.

7.2 Conclusion

This thesis discusses a V2L inverter and presented a methodology for integrating this single-phase V2L inverter into a three-phase nano-grid equipped with PV generation and battery storage. The existing system, based on SMA technology, comprises three Sunny Boys (SBs) and three Sunny Islands (SIs), all managed by a Data Manager (DM). Due to the inability of the V2L inverter to connect directly to the three-phase system, a new scheme was developed using a spare SI, an ioLogik, relays, and an alarm. It was selected among a few options that were discussed in the thesis.

This setup enables the implementation of load shedding and the supplementation of the stationary battery with energy from the EV, effectively extending the supply duration of the level 1 priority load during grid faults or islanded conditions. The control logic leverages the state of charge (SoC) of the stationary battery, which is shared among all system components via the DM. This approach strikes a balance between maintaining power supply to level 1 and, if possible, level 2 priority loads while conserving the EV's stored energy for critical situations.

Experimental results validate the feasibility and functionality of the proposed algorithm and the implemented scheme.

7.3 Summary of Chapters 1 to 6

Chapter 1: This chapter highlights the significance of this research by providing a concise overview of the integration of renewable energy systems in buildings, the role of EVs, and their interaction with the electrical grid, buildings, and homes.

Chapter 2: This chapter offered a comprehensive analysis of the Future Buildings Lab (FBL), including a detailed look at the building's infrastructure and the loads connected to the system.

Chapter 3: This chapter provided a detailed outline of the specifications for the electrical components used in the test system at the Future Buildings Lab (FBL). These components include the PV arrays, PV inverters, battery bank, battery inverters, SMA Data Manager M, ioLogik E1242, electric vehicle (EV), and SETEC inverter.

Chapter 4: This chapter examined the electrical and data connections of the components discussed in Chapter 3 to form the Experimental Setup. It also addressed the limitations encountered during the preparation and execution of the test setup, followed by a detailed explanation of the corresponding solutions implemented to overcome these challenges.

Chapter 5: This chapter covered the proposed procedure for utilizing the EV battery to support the AC nano-grid during critical utility outage conditions, as well as the energy management strategy employed to achieve this objective.

Chapter 6: This chapter presented the practical test results obtained from running the test setup with the implemented energy management strategy, validating the effectiveness of the proposed approach.

7.4 Future Work

In this research, a comprehensive experimental setup was developed and implemented, with the V2L test successfully carried out to demonstrate its functionality. Additionally, an alternative scheme together with a V2G configuration based on the original experimental setup was discussed in detail.

The versatility of this experimental setup extends beyond the demonstrated applications. It can accommodate other energy sources, such as fuel cells, wind turbines, and even additional PV systems, by connecting them to the DC bus.

These sources are planned for installation at the FBL; however, as of the time of this work, they have either not been installed or are not fully functional.

Future work could focus on the development of tailored protection interfaces for each energy sources to ensure safe and efficient integration. For instance, in case of wind turbine, when the stationary battery is fully charged to protect it against overcharge user cannot just disconnect wind turbine from DC bus. Here, a power dispute system is necessary. This would enhance the system's flexibility and expand its potential applications, making it a robust platform for advanced energy management and renewable energy research.

This work can be further expanded to include the development of a **comprehensive protection interface** combined with an **energy management strategy**. Such an approach would enable the integration of multiple energy sources—including fuel cells, wind turbines, PV systems, EVs, and others—simultaneously or in various combinations within the system.

This expanded framework would:

1. **Enhance System Flexibility**: Allow seamless connection and coordination of diverse energy sources, optimizing their combined contribution to the grid or nano-grid.

2. **Improve Energy Management**: Ensure efficient allocation of power to meet load demands while maintaining the stability and reliability of the system.

3. **Ensure Safety**: Provide robust protection mechanisms tailored to the unique characteristics of each energy source, preventing Over charging/ over discharging the battery, overloading power sources, and other potential issues.

4. **Support Scalability**: Create a modular system capable of accommodating additional sources as the energy infrastructure evolves.

By implementing these enhancements, the experimental setup could become a powerful platform for studying and deploying advanced, multi-source energy systems, further contributing to the advancement of renewable energy integration and energy resilience.

Note: it should be considered that in case of fully charged battery, the Dc power delivered to DC bus should be transferred to the Utility Grid through SIs. Thus, the total DC power connected to the DC bus should be limited to the total capacity of SIs.

References

[1] M. Lenox, R. Duff, “The decarbonization imperative: transforming the global economy by 2050,” Stanford Business Books, an imprint of Stanford University Press, Chapter 1, 2021.

[2] S. Attia, “Net zero energy buildings (NZEB): concepts, frameworks and roadmap for project analysis and implementation” Elsevier, 2018.

[3] M. Hu, “Net Zero Energy Building predicted and unintended consequences”, Routledge, 2019.

[4] “Homes and buildings”, https://www.canada.ca/en/services/environment/weather/climatechange /climate-action/federal-actions-clean-growth-economy/homes-buildings.html

[5] Z. Asadi, A. M. Aljehaimi, P. Pillay, "Solar Power Electronics System Design for the Future Building Laboratory at Concordia University," 2023 IEEE 14th International Conference on Power Electronics and Drive Systems (PEDS), Montreal, QC, Canada, 2023, pp. 1-6, doi: 10.1109/PEDS57185.2023.10246500.

[6] "Bibliothèque de Varennes,", https://biblio.ville.varennes.qc.ca/

[7] M. Abtahi, A. Athienitis, B. Delcroix, "Control-oriented thermal network models for predictive load management in Canadian houses with on-Site solar electricity generation: application to a research house," Journal of Building Performance Simulation, 2021.

[8] A. El-Shahat, “Nano-grid Technology Increasing, Supplementing Microgrids,” Natural Gas & Electricity, vol. 33, pp. 3–7, 2016.

[9] D. Borge-Diez, D. Icaza, E. Açıkkalp, H. Amaris.” Combined vehicle to building (V2B) and vehicle to home (V2H) strategy to increase electric vehicle market share”. Elsevier, Energy 237, 2021

[10] D. Mazzeo, N. Matera, R. De Luca, R. Musmanno, “A smart algorithm to optimally manage the charging strategy of the Home to Vehicle (H2V) and Vehicle to Home (V2H) technologies in an off-grid home powered by renewable sources”, Springer, Energy Systems, 2022.

[11] J. Lu, J. Hossain, “Vehicle-to-Grid: Linking Electric Vehicles to the Smart Grid”, IET POWER AND ENERGY SERIES 79, The Institution of Engineering and Technology, 2015.

[12] R. Shi, S. Peng, T. Chang, K. Y. Lee, “ Annotated Survey on the Research Progress within Vehicle-to-Grid Techniques Based on CiteSpace Statistical Result”, World Electric Vehicle Journal ,2023, https://www.mdpi.com/2032-6653/14/11/303.

[13] Liu, C., Chau, K. T., Wu, D., & Gao, S. (2013). Opportunities and Challenges of Vehicle-to-Home, Vehicle-to-Vehicle, and Vehicle-to-Grid Technologies. Proceedings of the IEEE, 101(11), 2409–2427. doi:10.1109/jproc.2013.2271951

[14] T. Osmancik, A. M. Aljehaimi and P. Pillay, "An Electric Vehicle Circuit for Powering Independent Loads," 2023 IEEE 14th International Conference on Power Electronics and Drive Systems (PEDS), Montreal, QC, Canada, 2023, pp. 1-5, doi: 10.1109/PEDS57185.2023.10268828.

[15] “6KW V2H Device Convert Battery Power Home Use Charger For Nissan Leaf Portable Chademo Charger”, httpswww.globalsources.comproductv2h_1209927359f.htm

[16] S. B. Slama, “Design and implementation of home energy management system using vehicle to home (H2V) approach”. Elsevier, Journal of Cleaner Production 312, 2021.

[17] I. Skouros, A. Karlis, “Design Methodology of a DC Nano-grid incorporating the V2G Technology”, IECON 2019 - 45th Annual Conference of the IEEE Industrial Electronics Society, pp. 5777 - 5782, 2019.

[18] K. C´ardenas, L. Reyes-Chamorro, N. Muller, M. D´ıaz, "V2H Charger Capable of Providing Ancillary Services", 2023 IEEE CHILEAN.

[19] H. Cheng, H. Chen, Q. Wang, "An Integrated Drive Power Converter Topology for Plug-in Hybrid Electric Vehicle with G2V, V2G and V2H Functions", 22nd International Conference on Electrical Machines and Systems (ICEMS), IEEE, 2019.

[20] "Bi-directional Charger (V2G/V2H)", https://www.deltathailand.com/en/products/Infrastructure/Energy/EV-Charging/AC-Charger/V2G

[21] "The All-New 2023 Nissan Leaf", https://www.nissan.ca/vehicles/electric-cars/leaf.html.

[22] "MITSUBISHI MOTORS IMPLEMENT FIRST 'VEHICLE TO GRID' PILOT ON DUTCH MARKET WITH MITSUBISHI OUTLANDER PHEV", https://www.mitsubishi-motors.com/en/newsrelease/2017/detail1082.html.

[23] "What's Bidirectional Charging and Which EVs Offer It?", https://www.cars.com/articles/whats-bidirectional-charging-and-which-evs-offer-it-457608/

[24] "Prepare for power outages", https://www.getprepared.gc.ca/cnt/hzd/pwrtgs-en.aspx

[25] "Blackout Tracker Canada Annual Report 2017", Annual Report 2017, www.powerquality.eaton.com/canada

[26] M. F. Hordeski, '' Emergency and Backup Power Sources: Preparing for Blackouts and Brownouts'", River Publishers, 2020.

[27] W. Zhang, Y. Wang, P. Xu, D. Li, and B. Liu, "Evaluation and Improvement of Backup Capacity for Household Electric Vehicle Uninterruptible Power Supply (EV-UPS) Systems", Energies 2023, 16,4567. https://doi.org/10.3390/en16124567

[28] K. M. Tan, V. K. Ramachandaramurthy, J. Y. Yong, "Integration of electric vehicles in smart grid: A review on vehicle to grid technologies and optimization techniques." Renewable and Sustainable Energy Reviews, P 720-732, 2016.

[29] M. El Chehaly, O. Saadeh, C. Martinez, G. Joos, "Advantages and applications of vehicle to grid mode of operation in plug-in hybrid electric vehicles," 2009 IEEE Electrical Power & Energy Conference (EPEC), Montreal, QC, Canada, P 1-6, 2009.

[30] S.M. Mousavi, F. Faraji, A. Majazi, K. Al-Haddad, "A comprehensive review of Flywheel Energy Storage System technology", Renewable and Sustainable Energy Reviews. P 477-490, 2017.

[31] M. Panteli, and P. Mancarella, "*The Grid: Stronger, Bigger, Smarter?*", ieee power & energy magazine, p 59-66, 2015.

[32] D. A. Reed, K. C. Kapur, and R. D. Christie, "Methodology for Assessing the Resilience of Networked Infrastructure", IEEE SYSTEMS JOURNAL, VOL. 3, NO. 2, JUNE 2009.

[33] J. Y. Heo, ... J. I. Lee "Evaluation of various large-scale energy storage technologies for flexible operation of existing pressurized water reactors", Nuclear Engineering and Technology , 2021

[34] Sunny Boy- SMA - SB7.7-1SP-US-41, https://shop.frankensolar.ca/sma-sb7-7-1sp-us-41/?srsltid=AfmBOorrpdRCh_KoMjmnucBcLU7QJ4A7n1ruvk9a5TdyxWzguwLAzB-C

[1] [35] PYLONTECH-US3000C Li-ion Battery, https://en.pylontech.com.cn/products/c23/121.html

[36] Sunny Island 6048-US, https://www.sma-america.com/products/battery-inverters/sunny-island-4548-us-6048-us

[37] "solar panel talk", https://www.solarpaneltalk.com/forum/solar-panels-for-home/solar-panel-installation/15286-sma-sunny-boy-sunny-island-help

[40] Data Manager M powered by ennexOS, https://www.sma-america.com/products/monitoring-control/data-manager-m-20

[39] ioLogik E1200 Series User's Manual, https://www.moxa.com/Moxa/media/PDIM/S100000327/moxa-iologik-e1200-series-manual

[40] SETEC Power Inverter, https://www.setec-power.com/

[41] Nissan Leaf 2015, https://www.cars.com/research/nissan-leaf-2015/

[42] Grizzl-E mini level 1-2 EV charger, https://grizzl-e.com

[43] Chroma 63802 programmable AC/DC electronic load, https://www.chromausa.com/product/programmable-ac-electronic-load-63800/